LEVEL II

SGI-R-79-011

5

SEISMIC WAVEFORM ANALYSIS OF UNDERGROUND NUCLEAR EXPLOSIONS

R. Butler
L. J. Ruff
R. S. Hart
G. R. Mellman

Annual Technical Report

Sponsored By

Advanced Research Projects Agency (DOD)
ARPA Order No. 3291-21
Monitored By AFOSR Under Contract #F49620-79-C-0012

November 15, 1979

SIERRA GEOPHYSICS, INC.
150 N. SANTA ANITA AVENUE • ARCADIA, CALIFORNIA 91006 • (213) 574-7052

ARPA Order: 3291-21

Program Code: 9F10

Effective Date of Contract: October 1, 1978

Contract Expiration Date: September 30, 1979

Amount of Contract: $74,994

Contract No. F49620-79-C-0012

Principal Investigators and Phone No.:

Dr. R. Butler

Dr. R. S. Hart

(213) 574-7052

Program Manager and Phone No.:

Mr. William J. Best (202) 767-4908

UNCLASSIFIED

SECURITY CLASSIFICATION OF THIS PAGE (When Data Entered)

(19) REPORT DOCUMENTATION PAGE	READ INSTRUCTIONS BEFORE COMPLETING FORM
(18) 1. REPORT NUMBER: AFOSR TR-79-1318	2. GOVT ACCESSION NO. / 3. RECIPIENT'S CATALOG NUMBER
(6) 4. TITLE (and Subtitle): SEISMIC WAVEFORM ANALYSIS OF UNDERGROUND NUCLEAR EXPLOSIONS,	5. TYPE OF REPORT & PERIOD COVERED: Scientific Interim
	6. PERFORMING ORG. REPORT NUMBER
(10) 7. AUTHOR(s): R. Butler, L. J. Ruff, R. S. Hart, G. R. Mellman	8. CONTRACT OR GRANT NUMBER(s): (15) F49620-79-C-0012 / DARPA Order-3291
9. PERFORMING ORGANIZATION NAME AND ADDRESS: Sierra Geophysics, Inc. 150 N Santa Anita Ave. Arcadia, CA 91006 (14) SGI-R-79-011	10. PROGRAM ELEMENT, PROJECT, TASK AREA & WORK UNIT NUMBERS: 62701E 9F10 A.O. 3291-21
11. CONTROLLING OFFICE NAME AND ADDRESS: DARPA/NMR 1400 Wilson Blvd. Arlington, VA 22209 (12) 81	12. REPORT DATE: (11) 15 Nov 1979
	13. NUMBER OF PAGES: 77
14. MONITORING AGENCY NAME & ADDRESS(if different from Controlling Office): AFOSR/NP Bolling AFB Wash DC 20332	15. SECURITY CLASS. (of this report): unclassified
	15a. DECLASSIFICATION/DOWNGRADING SCHEDULE

16. DISTRIBUTION STATEMENT (of this Report)

Approved for public release; distribution unlimited.

17. DISTRIBUTION STATEMENT (of the abstract entered in Block 20, if different from Report)

(9) Annual technical rept.,

18. SUPPLEMENTARY NOTES

19. KEY WORDS (Continue on reverse side if necessary and identify by block number)

The present research program

20. ABSTRACT (Continue on reverse side if necessary and identify by block number)

The research program discussed in this report represents an application of the methodologies of time domain seismology to the obseved short period P-waves from underground explosions. The goals of this program were to obtain better estimates of of the variation of short period seismic attenuation across the continental United States, evaluate the influence of different source regions on teleseismic P-wave amplitudes and waveforms, quantify the concepts of station/receiver transparency, and develop the initial states of a waveform inversion technique for both source discrimination and source description applications.

DD FORM 1 JAN 73 1473 EDITION OF 1 NOV 65 IS OBSOLETE

UNCLASSIFIED 393 821

A significant portion of the work performed on the first and second parts of this task was reported in the Sierra Geophysics Quarterly Technical Reports SGI-R-79-001 and SGI-R-79-004 submitted to the Air Force Office of Scientific Research. That research is summarized and some additional work and insights into the implications of the results are included. Sections contain discussions of station transparencies and progress report on waveform inversion techniques.

Accession For	
NTIS GRA&I	X
DDC TAB	
Unannounced	
Justification	
By	
Distribution/	
Availability Codes	
Dist.	Avail and/or special
A	

Sierra Geophysics, Inc.

150 N. Santa Anita Ave. • Suite 880 • Arcadia, California 91006 • (213) 574-7052

SGI-R-79-011

SEISMIC WAVEFORM ANALYSIS OF UNDERGROUND NUCLEAR EXPLOSIONS

R. Butler
L. J. Ruff
R. S. Hart
G. R. Mellman

Annual Technical Report

Sponsored By

Advanced Research Projects Agency (DOD)

ARPA Order No. 3291-21

Monitored By AFOSR Under Contract #F49620-79-C-0012

November 15, 1979

TABLE OF CONTENTS

I. INTRODUCTION

The research program discussed in this report represents an application of the methodologies of time domain seismology to the observed short period P-waves from underground explosions. The goal of this program was to obtain better estimates of the variation of short period seismic attenuation across the continental United States, evaluate the influence of different source regions on teleseismic P-wave amplitudes and waveforms, quantify the concepts of station/receiver transparency, and develop the initial stages of a waveform inversion technique for both source discrimination and source description applications. A significant portion of the work performed on the first and second parts of this task has been reported previously in the Sierra Geophysics Quarterly Technical Reports SGI-R-79-001 and SGI-R-79-004 submitted to the Air Force Office of Scientific Research. That research is summarized in Section II of this report and some additional work and insights into the implications of the results are included. Sections III and IV contain discussions of station transparencies and a progress report on waveform inversion techniques.

II. ANALYSIS OF SHORT PERIOD P-WAVE AMPLITUDES

Systematic studies of short period P-wave amplitudes from both underground nuclear explosions and simple earthquakes as recorded at WWSSN stations across North America have been conducted in order to investigate variations in receiver attenuation and bias introduced in the source region. For this purpose, data was collected from three primary source regions; first, nuclear explosions inside the Soviet Union which represent azimuths essentially due north from the United States; second, earthquakes in a northwestern azimuthal window from the U. S. (These sources are thus scattered along an arc stretching from Alaska, to the Aleutians, to Kamchatka and the Kurile Islands, to Japan the Bonin Islands); and third, South American events at a southeastern azimuth. Tables 1, 2, and 3 list the event data for these three azimuths. Underground nuclear explosions represent the ideal source for this type of study, since such sources have a theoretically isotropic radiation pattern. Earthquakes, on the other hand, exhibit strong radiation patterns which greatly reduces their utility. However, by careful selection of sources, one can minimize the effect of the radiation pattern and useful data can be obtained. We have examined a very large set of possible earthquake sources in the appropriate magnitude range (~5.5-6.0) in order to find an appropriate subset for this analysis. The criteria for this selection is principally a requirement that the short period P-waves are qualitatively simple, or bomb-like, in character all across the continental United States. This, of course, requires that the P-waves do not change polarity or vary significantly in waveform across the region. This selection process yielded a data set consisting of 36 nuclear explosions, 22 earthquakes from the northwest and 16 earthquakes from

Table 1

Explosion Data Set*

Northern Novaya Zemlya			
27 Oct 66	5:57:58	73.44N	54.75E
21 Oct 67	4:59:58	73.37N	54.81E
7 Nov 68	10:02:05	73.40N	54.86E
14 Oct 69	7:00:06	73.4PN	54.81E
14 Oct 70	6:02:57	73.31N	55.15E
27 Sept 71	5:59:55	73.39N	55.10E
28 Aug 72	5:59:57	73.34N	55.08E
12 Sept 73	6:59:54	73.30N	55.16E
29 Aug 74	9:59:56	73.37N	55.09E
23 Aug 75	8:59:58	73.37N	54.64E
21 Oct 75	11:59:57	73.35N	55.08E
Southern Novaya Zemlya			
27 Sept 73	6:59:58	70:76N	53.87E
2 Nov 74	4:59:57	70:82N	54.06E
18 Oct 75	8:59:56	70:84N	53.69E
Semipalatinsk East			
15 Jan 65	5:59:59	49.89N	78.97E
30 Nov 69	3:32:57	49.92N	79.00E
2 Nov 72	1:26:58	49.91N	78.84E
23 Jul 73	1:22:58	49.99N	78.85E
14 Dec 73	7:46:57	50.04N	79.01E
31 May 74	3:26:57	49.95N	78.84E
4 Jul 76	2:56:58	49.91N	78.95E
Semipalatinsk East-Additional Data			
23 Nov 76	5:03:00	50.00N	79.00E
12 Dec 76	4:57:00	49.90N	78.90E
29 May 77	2:59:00	49.9N	78.90E

Table 1 (continued)

Semipalatinsk West			
19 Oct 66	3:57:58	49.75N	78.03E
20 Apr 67	4:07:58	49.74N	78.12E
17 Oct 67	5:03:58	49.82N	78.10E
29 Sept 68	3:42:58	49.77N	78.19E
28 Jun 70	1:57:58	49.83N	78.25E
22 Mar 71	4:32:58	49.74N	78.18E
25 Apr 71	3:32:58	49.82N	78.09E
30 Dec 71	6:20:58	49.75N	78.13E
20 Feb 75	5:32:58	49.82N	72.08E
Kazakh			
6 Dec 69	7:02:57	43.83N	54.78E
12 Dec 70	7:00:57	43.85N	54.77E
23 Dec 70	7:00:57	43.83N	54.85E

*Locations and origin times from Dahlman and Israelson (1977)

TABLE 2

Earthquakes in a Northwest Azimuth

Date	Origin Time	Location	Depth (km)
Kurile Islands Earthquakes			
11/22/66	6:29:52.4	48.0N 14' 8E	441
3/20/67	12:31:34.0	45.6N 151.4E	51
8/10/67	11:21:22.3	45.4N 150.3E	37
2/10/68	10:00:05.8	46.0N 152.3E	87
4/28/68	4:18:15.7	44.8N 174.5E	39
7/25/68	10:50:31.5	45.7N 146.7E	16
10/26/76	5:58:56	46.1N 159.7W	130
3/19/77	10:56:06	43.0N 149.0E	0
Japanese Earthquakes			
1/1/77	11:33:42	30.6N 137.2E	483
1/5/77	22:44:57	23.3N 143.8E	0
2/18/77	20:51:26	34.0N 143.0E	0
6/12/77	8:48:05	43.0N 142.3E	241
Bonin Islands Earthquakes			
9/22/76	8:20:28	23.3N 142.1E	110
12/5/76	22:01:22	23.0N 140.0E	393
12/22/76	1:01:42	24.0N 145.0E	0
1/5/77	22:44:57	23.3N 143.8E	0

TABLE 2 continued

Earthquakes in a Northwest Azimuth

Date	Origin Time	Location	Depth (km)	Region
Other Events				
10/22/76	18:35:24	56.1N 153.3W	0	Kodiak Islands
4/22/77	5:58:56	52.5N 138.8E	408	Kamchatka
4/23/77	0:52:05	75.0N 134.9E	0	New Siberian Is.
7/20/77	14:49:06	50.6S 161.9W	0	Alaska Pen.
8/7/77	23:26:55	52.2N 176.2W	125	Andreanof Is.

TABLE 3

South American Earthquakes

Date	Origin Time	Location		Depth (km)
4/25/67	10:26:14.3	32.6N	69.0W	39
11/15/67	21:35:51.5	28.7S	71.2W	15
2/6/67	11:19:23.1	28.5S	71.0W	23
4/21/68	9:24:35.5	23.4S	70.5W	41
4/30/68	23:51:17.9	38.4S	71.1W	40
9/30/76	8:04:11	24.2S	68.2W	0
12/3/76	5:27:34	21.0S	69.0W	79
12/4/76	12:32:35	20.0S	69.0W	103
3/8/77	22:46:44	8.0S	63.0W	0
3/13/77	4:55:55	2.0S	58.0W	0
4/15/77	23:35:38	22.9S	68.8W	109
6/2/77	16:50:36	29.9S	68.6W	94
6/5/77	2:46:07	24.0S	70.5W	30
6/8/77	13:25:16	22.1S	67.3W	135
6/18/77	16:49:42	21.0S	68.7W	125

South America. A detailed description of the amplitude study of the Soviet nuclear events is contained in the report by Butler (1979). We will briefly review those results and then concentrate on the earthquake studies.

Evernden and Clark (1970) and Booth, Marshall and Young (1974) determined magnitude anomalies for Long Range Seismic Measurement (LRSM) stations in the United States and found that short period (1 sec) magnitudes of earthquakes measured at stations in the western United States, approximately west of the eastern front of the Rocky Mountains, are about 0.5 magnitude units (a factor of 3) smaller than magnitudes measured at stations in the central and eastern United States. The interpretation of this result has been that attenuation or dissipation of seismic energy is greater in the western United States than in the central and eastern United States. Consequently, it has been inferred that yields of explosions in the western United States must be corrected for this effect before comparison with other test sites. However, the results of Evernden and Clark (1970) and Booth et al. (1974) contain two sources of uncertainty. First, earthquake magnitudes were not corrected for the variations of radiation and the focusing effects characteristic of the earthquake source. Second, the manner in which m_b is typically measured does not lend itself to a straightforward comparison from one seismic station to another. The standard magnitude measure utilizes the maximum peak to peak amplitude within the first few seconds of the P-wave arrival and as a result, the same phase is not consistently measured from one station to the next.

The first task of our research program used short period P-wave amplitude variations observed at WWSSN stations in the United States from nuclear explosions from five test sites in the Soviet Union (see Figure 1). The

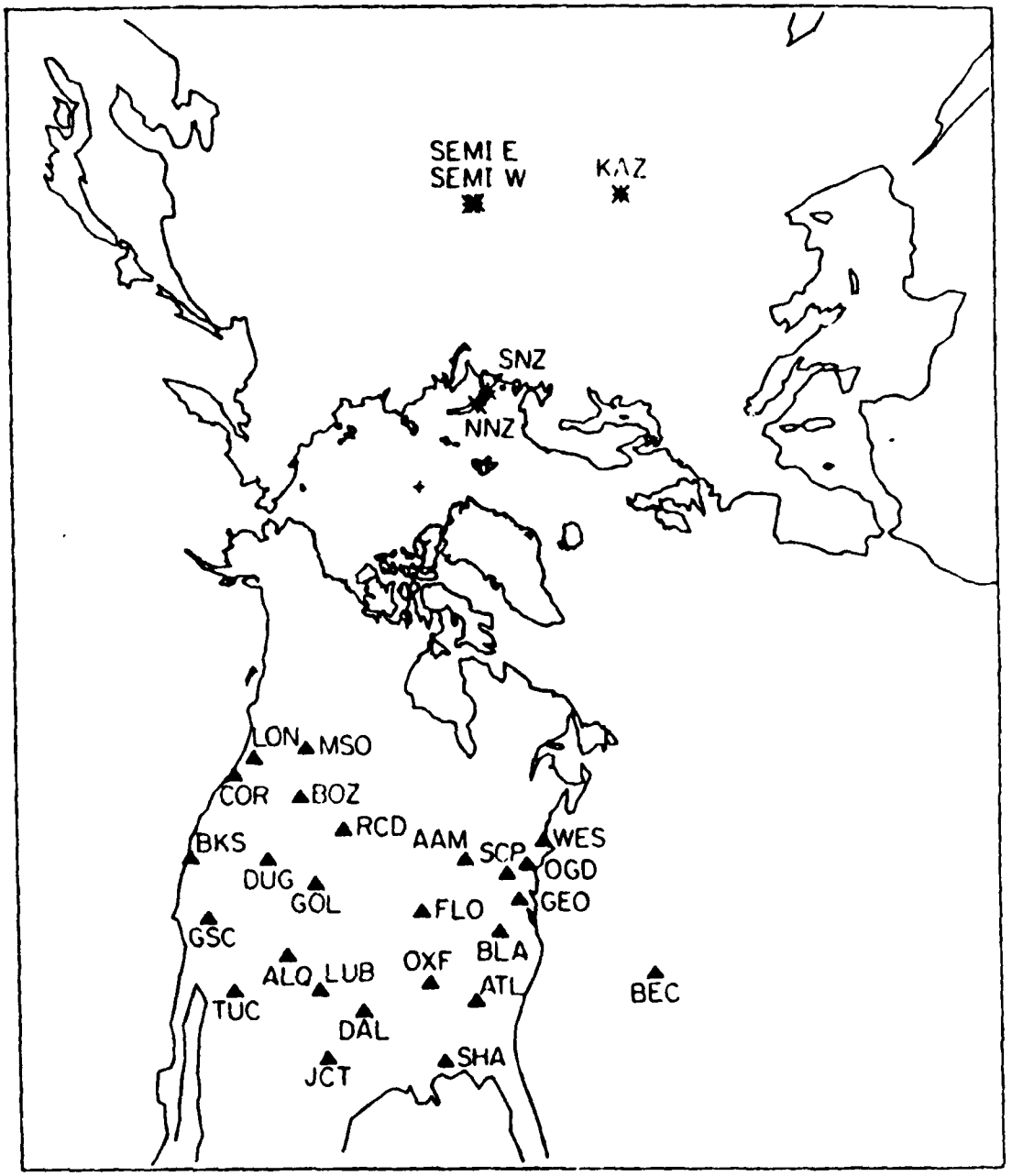

Figure 1: A gnomic projection (all great circles are straight lines) showing the source regions in the Soviet Union and the WWSSN stations in the United States.

symmetric explosion source is theoretically free of earthquake radiation variation and focusing effects. A consistent, specific amplitude measure is used which is related to the source strength, the so-called B-measurement (amplitude from first peak to first trough). Variations in observed amplitudes are interpreted as the result of both near source and near receiver effects. Although consistent amplitude variations are observed in the data, broad delineations, such as an eastern vs. western bias, are not supported by these data. The data show significant variation even within a single geologic province and suggest that amplitude characterizations of a single site cannot be assigned a priori on the basis of geologic province arguments. An excellent example of this is the SDCS station OB2-NV. Although the basin and range has been characterized by other investigators as highly attenuating, this NTS station reports amplitudes that are quite comparable with east coast stations.

In Figure 2, as well as other figures later in this report, the absolute source for each event amplitudes have been adjusted to minimize scatter using the following normalization procedure. From the i events choose a reference event k, to which the other events are to be scaled in a least squares sense. Scale factors α_i are determined such that the least squares error is minimized for each event $i \neq k$:

$$\min \Sigma \left|\alpha_i o_{ij} - o_{kj}\right|^2 \tag{1}$$

Let α_k be the average amplitude of the master event k:

$$\alpha_k = \frac{1}{j} \Sigma_j o_{kj} \tag{2}$$

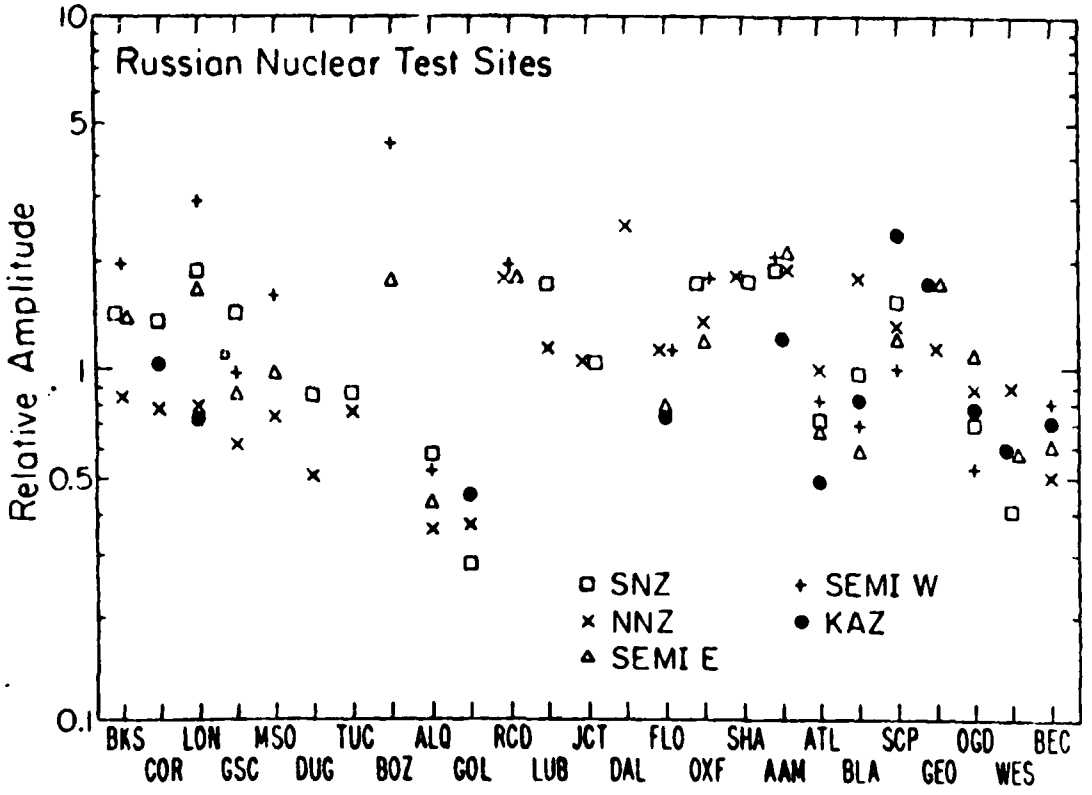

Figure 2: Combined plot of the amplitude data from the southern and northern Novaya Zemlya, east and west Semipalatinsk, and Kazakh sites for WWSSN stations across the United States. The mean of the amplitude data at each station for each site is plotted. Diffracted and anomalous (see text) data have been deleted.

The total error for all events i in the source region is then

$$\frac{1}{\alpha_k} \sum_i \sum_j |\alpha_i o_{ij} - o_{kj}|^2 \qquad (3)$$

We then iterate on the process, letting each event i in a source region be the master event k. The scale factors α_i in each source are chosen for the event k which minimizes the total error in (3) the best.

Tables 4 - 9 list the absolute amplitude determinations for the explosion data used in this study. Tables 10 - 16 list the average normalized amplitudes and standard error of the mean for the five Soviet test sites, individually and jointly.

The amplitude data from the five test sites (plotted in Figure 2) do not support the general results of Evernden and Clark (1970) and Booth et al. (1974) as the amplitudes for the stations in the western United States are comparable to the amplitudes of stations in the central and eastern United States.

The second phase of this task involved the analysis of the P-wave amplitudes from the earthquake data for the northwest and southeast azimuths. This task not only allowed us to augment the explosion data and hence build confidence in the results found there but also to examine the receiver function and amplitude patterns for azimuthally-dependent variations.

Tables 17 - 20 and 26 list the absolute amplitude measurements for the northwestern and southeastern azimuth data sets respectively. Tables 21 - 25 and Table 27 list the normalized station amplitudes and standard error of the mean for these same data sets. Examples of the simple P-wave earthquakes utilized in this study are contained in an earlier report

Table 4

Northern Novaya Zemlya Explosions

STATION	10/27/66	10/21/67	11/ 7/68	10/14/69	10/14/70
BKS	506.4	110.1	176.1	275.2	2113.8
COR	374.3	132.1	220.2	264.2	
LON			165.1	247.7	
GSC		57.8	159.6		
MSO					
DUG	385.3	66.1	118.3	166.5	1100.9
TUC		134.9	195.4	235.3	
BOZ					
ALQ	187.2	57.8	82.6	121.1	721.1
GOL	228.4	57.8	79.8	128.0	
RCD	1145.0				
LUB		209.2	242.2	418.3	
JCT		166.5	233.4		
DAL			638.5		
FLO					2267.9
OXF	990.8	203.7	308.3	451.4	2873.4
SHA	1321.1	308.3	396.3	616.5	3699.1
AAM	1453.2	330.3	418.3	506.4	2664.2
ATL	682.6	137.6			2058.7
BLA		269.7	412.8		
SCP		192.7	308.3	440.4	
GEO		132.1	286.2	418.3	2267.9
OBD		159.6	214.7	291.7	
WES		132.1	192.7	275.2	1541.3
BEC	308.3		110.1		

Table 4

Northern Novaya Zemlya Explosions (continued)

STATION	9/27/71	8/28/72	9/12/73	8/29/74	8/23/75
BKS	803.7		2752.3	616.5	605.5
COR		418.3		572.5	528.4
LON		412.8		638.5	682.6
GSC				605.5	
MSO					561.5
DUG				379.8	338.5
TUC	726.6	407.3			
BOZ					
ALQ		203.7		242.2	291.7
GOL					
RCD		990.8			
LUB			2763.3		
JCT					
DAL	2466.1	1365.1			
FLO					
OXF	1425.7		3313.8	1001.8	1012.8
SHA		836.7	5064.2	1189.0	1497.2
AAM	2069.7	1100.9			
ATL	946.8	550.5			
BLA					
SCP					
GEO					770.6
OGD	913.8			693.6	605.5
WES	990.8	572.5			
BEC	517.4	319.3		385.3	319.3

Table 4

Northern Novaya Zemlya Explosions (continued)

STATION	10/21/75
BKS	990.8
COR	880.7
LON	781.7
GSC	
MSO	737.6
DUG	
TUC	
BOZ	
ALQ	
GOL	
RCD	
LUB	
JCT	
DAL	
FLO	
OXF	1420.2
SHA	1717.4
AAM	
ATL	
BLA	
SCP	
GEO	1348.6
OGD	748.6
WES	
BEC	

Table 5

Southern Novaya Zemlya Explosions

STATION	9/21/73	11/ 2/74	10/18/75
BKS	220.2	2730.3	968.8
COR	176.1		1078.9
LON	267.0		
GSC	203.7		
MSO			
DUG	119.7		
TUC	121.1		
BOZ			
ALQ	81.2		
GOL	44.0	481.7	
RCD			
LUB	242.2		
JCT			754.1
DAL			
FLO			
OXF	258.7	3071.6	1315.6
SHA		3434.9	1233.0
AAM	242.2	4051.4	
ATL		1387.2	
BLA	123.9	2036.7	
SCP	214.7		
GEO			
OGD	88.1		561.5
WES		759.6	
BEC			

Table 6

Semipalitinsk East Explosions

STATION	1/15/65	11/30/69	11/ 2/72	7/23/73	12/14/73
BKS	86.8	55.3	126.3	142.1	55.3
COR		142.1		276.3	315.8
LON		71.1		146.1	63.2
GSC	51.3		80.9		
MSO					39.5
DUG					
TUC	10.9	6.9	15.8	17.8	4.4
BOZ	86.8				
ALQ	19.7	15.8		38.0	10.9
GOL	55.3	42.5	80.0		31.6
RCD	86.8				
LUB		31.6	63.2	63.2	
JCT		3.9	5.9	9.9	
DAL	78.9			118.4	
FLO	35.5	31.6			
OXF		39.5	102.6	150.0	
SHA					
AAM	118.4	63.2	165.8	244.7	110.5
ATL	31.6	23.7	59.2		
BLA	23.7	19.7	55.3	74.1	
SCP		55.3		102.6	
GEO	71.1	67.1			
OGD			98.7	130.3	39.5
WES			43.4	55.3	
BEC				63.2	

Table 6

Semipalitinsk East Fxplosions (continuted)

STATION	5/31/74	7/ 4/76
BKS		39.5
COR	78.9	86.8
LON	52.3	55.3
GSC	26.7	23.7
MSO	22.7	
DUG		100.7
TUC		5.0
BOZ		
ALQ		11.8
GOL	34.6	
RCD		
LUB		
JCT	7.4	
DAL		
FLO		
OXF		
SHA		
AAM	47.4	
ATL	23.7	
BLA	17.8	19.7
SCP		
GEO	47.4	67.1
OGD	39.5	27.6
WES	23.7	15.8
BEC		

Table 7

Additional Semipalitinsk East Explosions

STATION	11/23/76	12/ 7/76	5/29/77
BKS	61.1	55.6	
COR	178.6	111.1	132.1
LON			
GSC	38.9	38.9	33.0
OB2NV			63.8
MSO	50.0	44.4	35.8
DUG		147.2	123.9
TUC	8.3		6.9
BOZ			
ALQ	13.9	16.7	15.1
GOL	44.4	45.8	
LUB			
JCT			
DAL			
RKON	281.8	326.9	273.5
OXF			
SHA			
AAM			
ATL	33.3		33.0
BLA	44.4	41.7	22.0
SCP	77.8	50.0	55.0
GEO			110.1
OGD	44.4	50.0	49.5
WES			
HNME	132.3		112.6

Table 8

Semipalitinsk West Explosions

STATION	10/19/66	4/20/67	10/17/67	9/29/68	6/28/70
BKS	31.6	27.6	15.8	39.5	47.4
COR	78.9			110.5	86.8
LON	53.3	31.6	37.5	65.1	51.3
GSC	14.8	14.8	5.0		
MSO					
DUG			83.9		
TUC	3.5		1.0	3.9	6.4
BOZ		39.5	42.5		
ALQ	8.9	6.9	6.9	13.3	13.8
GOL	22.7	16.3	15.8	37.5	34.6
RCD	31.6				
LUB	15.8	11.8			
JCT	4.4		3.0		3.5
DAL				31.6	
FLO					
OXF	29.6		17.8	35.5	
SHA					
AAM	31.6	23.7		39.5	47.4
ATL	13.8		3.9	21.7	21.7
BLA				20.8	
SCP	11.8	11.8	5.9	19.7	27.6
GEO					
OGD				11.8	
WES					
BEC					

Table 8

Semipalitinsk West Explosions (continued)

STATION	3/22/71	4/25/71	12/30/71	2/20/75
BKS	31.6	63.2	43.4	
COR			110.5	
LON	43.4	78.9	65.1	
GSC				17.8
MSO				23.7
DUG				
TUC	3.5	7.9		3.5
BOZ				
ALQ	7.9			8.9
GOL	24.7	53.3	27.6	25.2
RCD				
LUB	15.8	39.5		18.9
JCT	5.4	13.8	3.9	3.9
DAL		55.3	31.6	
FLO		35.5		
OXF	31.6		35.5	21.7
SHA				
AAM	39.5	47.4	31.6	51.6
ATL		27.6	15.8	
BLA		19.7	13.8	7.9
SCP	19.7	43.4		
GEO				
OGD				
WES				
BEC				11.8

Table 9

Western Kazakh Explosions

STATION	12/ 6/69	12/12/70	12/23/70
BKS	17.5	28.1	21.2
COR	63.2	70.4	71.1
LON	35.7	60.0	55.3
GSC	3.5		
MSO			
DUG	19.4	30.8	25.3
TUC	1.6	4.9	6.2
BOZ			
ALQ	9.9	17.4	15.5
GOL	21.0	32.2	39.6
RCD			
LUB		33.2	25.3
JCT		7.1	11.1
DAL		40.4	
FLO	33.5		
OXF	83.8	150.8	123.5
SHA			
AAM	77.1	78.9	78.9
ATL	24.5	35.2	39.5
BLA	30.9	66.2	78.9
SCP	110.5	175.3	213.2
GEO	70.6	150.0	157.9
OGD	22.9	60.0	88.4
WES		48.2	
BEC			58.4

Table 10

Northern Novaya Zemlya

STATION	MEAN	S.E.M.	N
BKS	0.89	0.04	10
COR	0.82	0.04	8
LON	0.82	0.04	6
GSC	0.65	0.13	3
MSO	0.77	0.03	2
DUG	0.53	0.02	7
TUC	0.81	0.04	5
BOZ			
ALQ	0.37	0.01	8
GOL	0.38	0.01	4
RCD	1.84	0.00	2
LUB	1.23	0.10	4
JCT	1.10	0.06	2
DAL	2.63	0.11	3
FLO	1.18		1
OXF	1.43	0.03	10
SHA	1.89	0.07	10
AAM	1.95	0.13	7
ATL	1.02	0.03	5
BLA	1.86	0.02	2
SCP	1.37	0.01	3
GEO	1.19	0.07	6
OGD	0.92	0.04	7
WES	0.92	0.04	6
BEC	0.51	0.02	6

Table 11

Southern Novaya Zemlya

STATION	MEAN	S.E.M.	N
BKS	1.38	0.08	3
COR	1.31	0.09	2
LON	1.84		1
GSC	1.41		1
MSO			
DUG	0.83		1
TUC	0.84		1
BOZ			
ALQ	0.56		1
GOL	0.27	0.03	2
RCD			
LUB	1.67		1
JCT	0.98		1
DAL			
FLO			
OXF	1.67	0.07	3
SHA	1.66	0.06	2
AAM	1.85	0.18	2
ATL	0.69		1
BLA	0.94	0.08	2
SCP	1.48		1
GEO			
OGD	0.67	0.06	2
WES	0.38		1
BEC			

Table 12

Semipalitinsk East

STATION	MEAN	S.E.M.	N
BKS	1.52	0.05	6
COR	4.16	1.09	5
LON	1.75	0.07	5
GSC	0.93	0.05	4
MSO	0.91	0.15	2
DUG	3.51		1
TUC	0.18	0.01	6
BOZ	1.72		1
ALQ	0.38	0.02	5
GOL	1.04	0.06	5
RCD	1.72		1
LUB	0.76	0.05	3
JCT	0.13	0.04	4
DAL	1.40	0.16	2
FLO	0.77	0.07	2
OXF	1.30	0.15	3
SHA			
AAM	2.20	0.22	6
ATL	0.69	0.04	4
BLA	0.62	0.05	6
SCP	1.27	0.20	2
GEO	1.78	0.20	4
OGD	1.18	0.08	5
WES	0.61	0.06	4
BEC	0.66		1

Table 13

Semipalitinsk East Including Additional Events

STATION	MEAN	S.E.M.	N
BKS	1.26	0.05	8
COR	3.26	0.58	8
LON	1.52	0.06	5
GSC	0.77	0.03	7
OB2NV	1.34		1
MSO	0.82	0.05	5
DUG	2.83	0.12	3
TUC	0.15	0.01	8
BOZ	1.47		1
ALQ	0.32	0.02	8
GOL	0.89	0.04	7
LUB	0.67	0.05	3
JCT	0.12	0.03	4
DAL	1.21	0.13	2
RKON	5.75	0.37	3
OXF	1.14	0.13	3
SHA			
AAM	1.90	0.18	6
ATL	0.62	0.03	6
BLA	0.59	0.05	9
SCP	1.16	0.09	5
GEO	1.69	0.21	5
OGD	0.99	0.05	8
WES	0.53	0.05	4
HNME	2.38	0.02	2

Table 14

Semipalitinsk West

STATION	MEAN	S.E.M.	N
BKS	1.56	0.06	8
COR	3.74	0.26	4
LON	2.33	0.22	8
GSC	0.76	0.10	4
MSO	1.15		1
DUG	8.28		1
TUC	0.16	0.01	7
BOZ	3.38	0.82	2
ALQ	0.47	0.04	7
GOL	1.20	0.05	9
RCD	1.51		1
LUB	0.81	0.04	5
JCT	0.22	0.03	7
DAL	1.19	0.06	3
FLO	0.80		1
OXF	1.38	0.10	6
SHA			
AAM	1.58	0.16	8
ATL	0.63	0.05	6
BLA	0.52	0.07	4
SCP	0.78	0.07	7
GEO			
OGD	0.40		1
WES			
BEC	0.57		1

Table 15

Western Kazakh

STATION	MEAN	S.E.M.	N
BKS	0.65	0.07	3
COR	2.05	0.34	3
LON	1.44	0.06	3
GSC	0.15		1
MSO			
DUG	0.73	0.07	3
TUC	0.11	0.02	3
BOZ			
ALQ	0.41	0.02	3
GOL	0.88	0.05	3
RCD			
LUB	0.71	0.11	2
JCT	0.22	0.04	2
DAL	0.99		1
FLO	1.44		1
OXF	3.42	0.24	3
SHA			
AAM	2.38	0.47	3
ATL	0.95	0.05	3
BLA	1.62	0.16	3
SCP	4.72	0.23	3
GEO	3.50	0.23	3
OGD	1.52	0.33	3
WES	1.18		1
BEC	1.40		1

Table 16

Mean Normalized Amplitudes and Standard Error of the Mean for the Five Soviet Test Sites

STATION	MEAN	S.E.M.	N
BKS	1.10	0.14	4
COR	0.89	0.10	3
LON	1.27	0.28	5
GSC	0.75	0.11	4
OB2NV	1.22		1
MSO	0.87	0.16	3
DUG	0.54	0.09	2
TUC	0.66	0.02	2
BOZ	1.44		1
ALQ	0.37	0.04	4
GOL	0.32	0.06	3
LUB	1.15	0.12	2
JCT	0.85	0.08	2
DAL	2.23		1
RKON	4.89		1
OXF	1.19	0.08	4
SHA	1.44	0.15	2
AAM	1.48	0.10	5
ATL	0.60	0.07	5
BLA	0.81	0.20	5
SCP	1.26	0.25	5
GEO	1.40	0.20	3
OGD	0.65	0.09	5
WES	0.52	0.10	4
HNME	2.14		1

Table 17

Kurile Earthquakes

STATION	11/22/66	3/20/67	8/10/67	2/10/68	4/28/68
BKS		112.3	101.8	100.2	
COR	453.1			253.8	
LON	161.8		24.2		
GSC	417.8		66.1	67.7	
OB2NV					
MSO					
DUG	513.6	79.3	125.0	148.6	
TUC	340.4	36.9	59.4	71.0	
BOZ	508.6	64.4	143.1	238.3	
ALQ	298.7	25.9	65.0	52.8	
GOL	202.1	18.7	46.2	53.9	15.4
LUB	450.5			120.0	45.1
JCT	440.8	60.0			
DAL	744.2				95.2
RKON					
OXF	973.7	161.3	184.4	319.8	
SHA	496.7				
AAM	475.4		197.1	305.0	36.3
ATL	462.4	76.5	154.1	182.2	58.3
BLA	407.2	83.1	174.5	262.0	65.0
SCP	351.4	44.0	111.7	138.2	57.2
GEO	271.5				
OGD	222.9				
WES	435.2	104.6	181.1	191.6	
HNME					

Table 17

Kurile Earthquakes (continued)

STATION	7/25/68	10/26/76	3/19/77
BKS	138.7		912.7
COR	242.2		1388.3
LON			195.4
GSC		710.1	924.8
OB2NV			
MSO		842.2	1278.2
DUG	185.0	1178.0	1187.9
TUC	122.2	505.9	724.4
BOZ			
ALQ	149.7		
GOL		233.4	
LUB	251.6		1545.7
JCT			
DAL			1048.1
RKON			
OXF			
SHA			
AAM			4634.3
ATL		765.1	2174.3
BLA	146.4		2715.4
SCP			
GEO			1404.2
OGD	273.6		
WES	182.2		
HNME			

Table 18

Other Earthquakes to a Northwest Azimuth from the United States

STATION	10/22/76	4/22/77	4/23/77	7/20/77	8/ 7/77
BKS	44.8	53.4			85.9
COR					112.5
LON			21.6		
GSC				44.8	
OB2NV		52.4	26.7	68.5	54.8
MSO		65.4	14.7	26.6	105.2
DUG	45.6	70.9	21.1		
TUC	55.5	22.2	7.3	44.0	47.8
BOZ					
ALQ	31.5				
GOL	20.1	13.1			
LUB					
JCT		56.2	45.8		
DAL					97.1
RKON			30.3	146.2	
OXF					
SHA					
AAM					
ATL	35.6				
BLA				130.9	
SCP			14.7	105.7	
GEO	56.9				
OGD	49.8			37.7	
WES					
HNME				74.3	

Table 19

Japanese Earthquakes

STATION	12/31/76	1/ 1/77	2/18/77	6/12/77
BKS		196.1	734.2	
COR		186.7	323.6	
LON			118.3	
GSC	7.1	56.3	325.5	19.3
OB2NV	16.4			39.8
MSO	18.4	53.0	310.7	30.0
DUG	19.5	93.7	483.0	51.0
TUC	7.7	18.3		15.0
BOZ				
ALQ	12.4	37.0		30.0
GOL	9.7			
LUB				
JCT				
DAL				
RKON	44.6			50.7
OXF				
SHA				
AAM				
ATL				
BLA				
SCP				
GEO				
OGD				
WES				
HNME				

Table 20

Bonin Islands Earthquakes

STATION	9/22/76	12/ 5/76	12/22/76	1/ 5/77
BKS	212.2	98.8	339.8	
COR	106.8			
LON	48.6			37.0
GSC	148.8	79.3		157.5
OB2NV			210.3	
MSO	33.7		87.8	
DUG	277.8	115.0		124.7
TUC	51.1	22.5	132.7	60.5
BOZ				
ALQ	26.9	50.0	149.8	
GOL	52.5	12.2	62.1	
LUB			170.2	
JCT				
DAL				
RKON		179.9	315.8	
OXF				
SHA				
AAM				
ATL				
BLA				
SCP				
GEO				
OGD				
WES				
HNME				

Table 21

Kurile Islands

STATION	MEAN	S.E.M.	N
BKS	0.97	0.20	5
COR	1.34	0.17	4
LON	0.25	0.07	3
OSC	0.73	0.10	5
OB2NV			
MSO	1.00	0.01	2
DUG	1.14	0.06	7
TUC	0.61	0.04	7
BOZ	1.30	0.14	4
ALQ	0.58	0.09	5
GOL	0.37	0.03	6
LUB	1.13	0.09	5
JCT	1.01	0.07	2
DAL	1.64	0.43	3
RKON			
OXF	2.20	0.21	4
SHA	1.21		1
AAM	1.92	0.49	5
ATL	1.28	0.10	7
BLA	1.46	0.18	7
SCP	0.97	0.11	5
GEO	0.89	0.22	2
OGD	1.04	0.49	2
WES	1.33	0.13	5
HNME			

Table 22

Northwest Azimuth

STATION	MEAN	S.E.M.	N
BKS	0.96	0.16	3
COR	1.44		1
LON	1.39		1
GSC	0.77		1
OB2NV	1.18	0.21	4
MSO	1.04	0.22	4
DUG	1.17	0.27	3
TUC	0.62	0.07	5
BOZ			
ALQ	0.44		1
GOL	0.28	0.00	2
LUB			
JCT	2.07	0.87	2
DAL	1.24		1
RKON	2.23	0.28	2
OXF			
SHA			
AAM			
ATL	0.50		1
BLA	2.25		1
SCP	1.38	0.44	2
GEO	0.80		1
OGD	0.68	0.03	2
WES			
HNME	1.28		1

Table 23

Japan

STATION	MEAN	S.E.M.	N
BKS	2.74	0.33	2
COR	1.99	0.93	2
LON	0.39		1
GSC	0.74	0.14	4
OB2NV	1.11	0.09	2
MSO	0.98	0.07	4
DUG	1.45	0.08	4
TUC	0.41	0.06	3
BOZ			
ALQ	0.75	0.10	3
GOL	0.61		1
LUB			
JCT			
DAL			
RKON	2.16	0.62	2
OXF			
SHA			
AAM			
ATL			
BLA			
SCP			
GEO			
OGD			
WES			
HNME			

Table 24

Bonin Islands

STATION	MEAN	S.E.M.	N
BKS	2.07	0.21	3
COR	1.24		1
LON	0.51	0.05	2
GSC	1.77	0.11	3
OB2NV	1.09		1
MSO	0.42	0.03	2
DUG	2.37	0.48	3
TUC	0.62	0.07	4
BOZ			
ALQ	0.70	0.20	3
GOL	0.39	0.11	3
LUB	0.88		1
JCT			
DAL			
RKON	2.63	0.99	2
OXF			
SHA			
AAM			
ATL			
BLA			
SCP			
GEO			
OGD			
WES			
HNME			

Table 25

All Earthquakes To Northwest

STATION	MEAN	S.E.M.	N
BKS	1.26	0.16	13
COR	1.30	0.17	8
LON	0.38	0.10	7
GSC	0.76	0.08	13
OB2NV	0.91	0.06	7
MSO	0.75	0.09	12
DUG	1.18	0.10	17
TUC	0.51	0.04	19
BOZ	1.24	0.13	4
ALQ	0.57	0.05	12
GOL	0.34	0.03	12
LUB	1.02	0.09	6
JCT	1.22	0.24	4
DAL	1.42	0.28	4
RKON	1.77	0.20	6
OXF	2.09	0.18	4
SHA	1.14		1
AAM	1.84	0.49	5
ATL	1.14	0.11	8
BLA	1.44	0.16	8
SCP	0.95	0.11	7
GEO	0.92	0.15	3
OGD	0.85	0.22	4
WES	1.27	0.13	5
HNME	1.00		1

Table 26

South American Earthquakes

STATION	4/25/67	11/15/67	2/ 6/68	4/21/68	4/30/68
BKS	106.2	314.9	143.1		
COR		678.2	277.4		
LON	24.8	176.1	73.8		
GSC		255.4	113.9		142.0
OB2NV					
MSO					
DUG	69.4		233.9		146.4
TUC	50.1	166.2	75.4	53.9	96.9
BOZ		147.0			
ALQ	106.8	216.3	84.8	56.7	143.1
GOL	68.3	203.1	78.7		140.4
LUB	255.4		339.1	115.6	
JCT	238.3				
DAL	211.4				
RKON					
OXF	456.3	583.5	151.9		402.9
SHA					
AAM		401.8			142.0
ATL	227.9		56.7	53.9	367.2
BLA			47.3		
SCP	77.1	323.7	73.2	63.9	187.2
GEO	100.2	312.1			
OGD			61.1		270.3
WES			74.9		169.0
HNME					

Table 26

South American Earthquakes (continued)

STATION	9/30/76	12/ 3/76	12/ 4/76	3/ 8/77	3/13/77
BKS	120.3	86.7	107.6		
COR	214.7	186.2	143.3		
LON	59.9				
GSC	185.5	95.3	126.7	29.7	59.5
OB2NV					
MSO	100.9	49.4	75.8	62.8	
DUG	150.4	48.4	121.4	55.0	53.0
TUC	127.1	61.2	70.1		20.8
BOZ					
ALQ		54.9	42.7		
GOL		41.6	48.8		
LUB					103.3
JCT				27.8	
DAL					257.1
RKON			96.1		
OXF					
SHA					
AAM					
ATL	58.6	37.5		65.4	54:7
BLA		60.6		76.5	
SCP					
GEO				96.7	
OGD				34.2	18.6
WES					37.3
HNME					

Table 26

South American Earthquakes (continued)

STATION	4/15/77	6/ 2/77	6/ 5/77	6/ 8/77	6/18/77
BKS	177.6		82.6	151.4	203.1
COR			118.1	177.0	
LON	32.0	11.0	26.1		363.3
GSC		28.5	66.3	161.0	215.3
OB2NV	131.7	56.8	74.3	186.6	
MSO	93.4	13.8	98.7	116.2	
DUG		33.8	88.4	176.8	225.5
TUC	116.2	17.8	63.0	148.4	130.8
BOZ					
ALQ					
GOL					
LUB					
JCT					
DAL			67.4		
RKON	221.8	60.2	171.3		
OXF					
SHA					
AAM					
ATL	72.8		75.6	96.1	
BLA	83.7		89.9	264.2	
SCP					
GEO	72.5		68.1	77.9	
OGD			40.4	34.3	
WES					
HNME	125.6		85.8		

Table 27

STATION	MEAN	S.E.M.	N
BKS	1.09	0.08	10
COR	1.83	0.18	7
LON	0.52	0.13	8
GSC	0.99	0.09	12
OB2NV	1.39	0.18	4
MSO	0.87	0.10	8
DUG	1.07	0.12	12
TUC	0.69	0.07	14
BOZ	0.38		1
ALQ	0.68	0.06	7
GOL	0.58	0.03	6
LUB	2.15	0.31	4
JCT	1.26	0.76	2
DAL	2.53	1.20	3
RKON	1.85	0.30	4
OXF	2.10	0.59	4
SHA			
AAM	0.81	0.22	2
ATL	0.94	0.14	11
BLA	1.11	0.23	6
SCP	0.75	0.04	5
GEO	0.94	0.17	6
OGD	0.58	0.12	6
WES	0.69	0.02	3
HNME	1.18	0.00	2

(Butler and Hart, 1979). The data tabulated in the above tables are displayed graphically in Figures 3 - 9. Figures 3 and 4 plot the normalized explosion data and the mean of that data for the five Soviet test sites. The data shows remarkably low scatter (less than a factor of 2) except for two prominently low stations, ALQ and GOL both located in the Rocky Mountain province. The other particularly noticeable anomalous station is RKON, an SDCS station located on the Canadian shield. A detailed discussion of this station as well as the other SDCS stations OB2-NV and HNME on this and other figures in this report can be found in Hart et al. (1979) and will not be considered here. If these seemingly anomalous data points are disregarded, no systematic regional bias in short period amplitudes can be discerned.

Figures 5 and 6 are similar in kind to the preceding pair of figures but, in this case, the data are amplitudes observed from earthquakes to the northwest. Again the stations ALQ and GOL are low. Station LON in Washington is also anomalously low but previous studies (Langston, 1976) have shown that this station has an extreme azimuthal dependence in its receiver function due to dips in the local crustal structure. Without these data, once again regional correlations in amplitudes are not significant.

Figures 7 and 8 illustrate data from South American events, incident from a southeastern azimuth. In this example, the stations at Albuquerque and Golden are not noticeably low indicating that the "problems" with those stations may result from deep structure beneath the central Rocky Mountain front (see Hadley, 1979). P-waves incident from this azimuth do show a quite noticeable regional pattern. Specifically, WWSSN stations in the central midwest (LUB, JCT, DAL, OXF) show much high (factor of ~3) amplitudes than stations either farther east or farther west. The eastern and

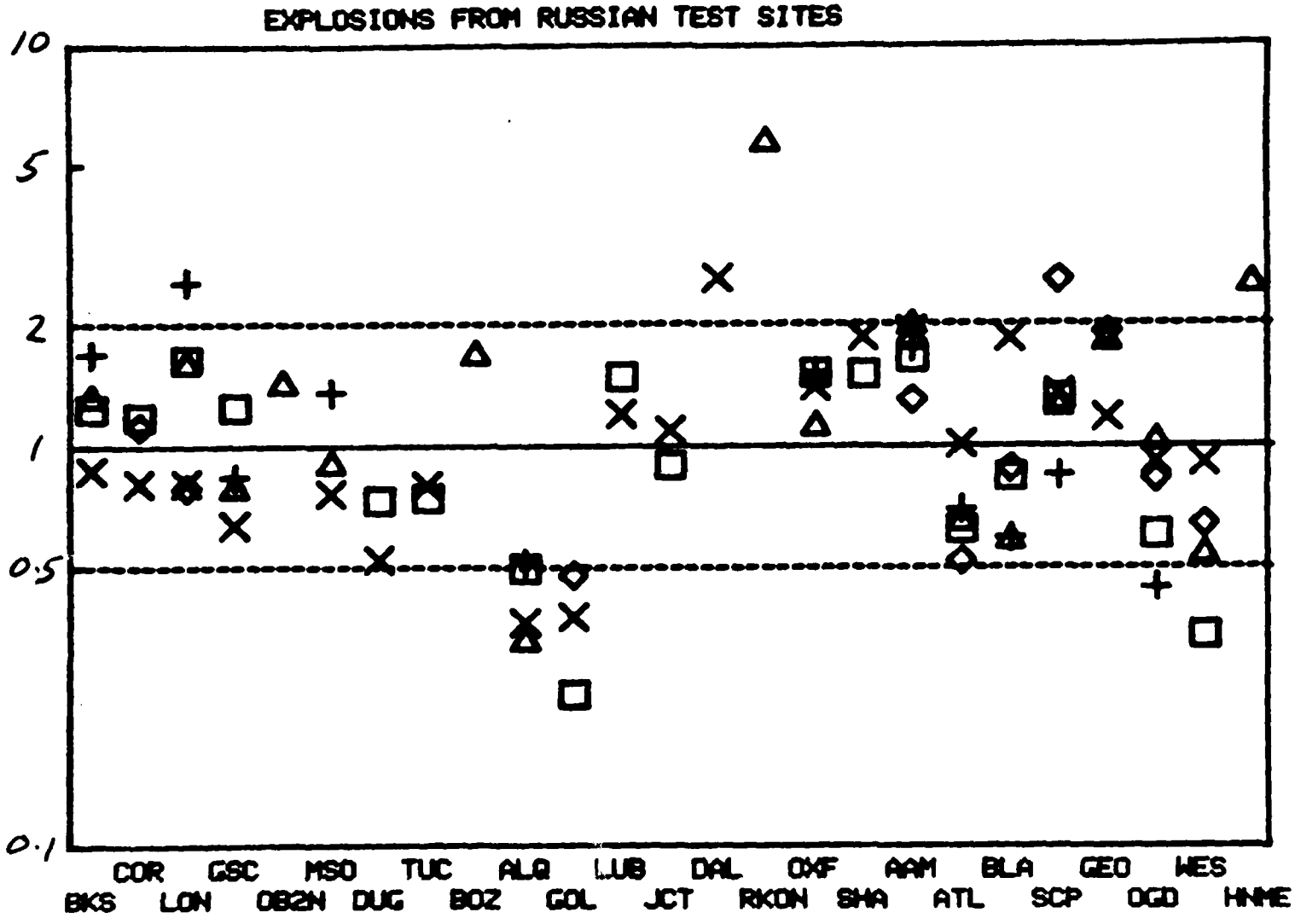

Figure 3. Mean amplitude data from the five Soviet test sites.

(Box - SNZ; X-NNZ; Diamond - KAZ; Triangle - Semi U; and cross - Semi-U)

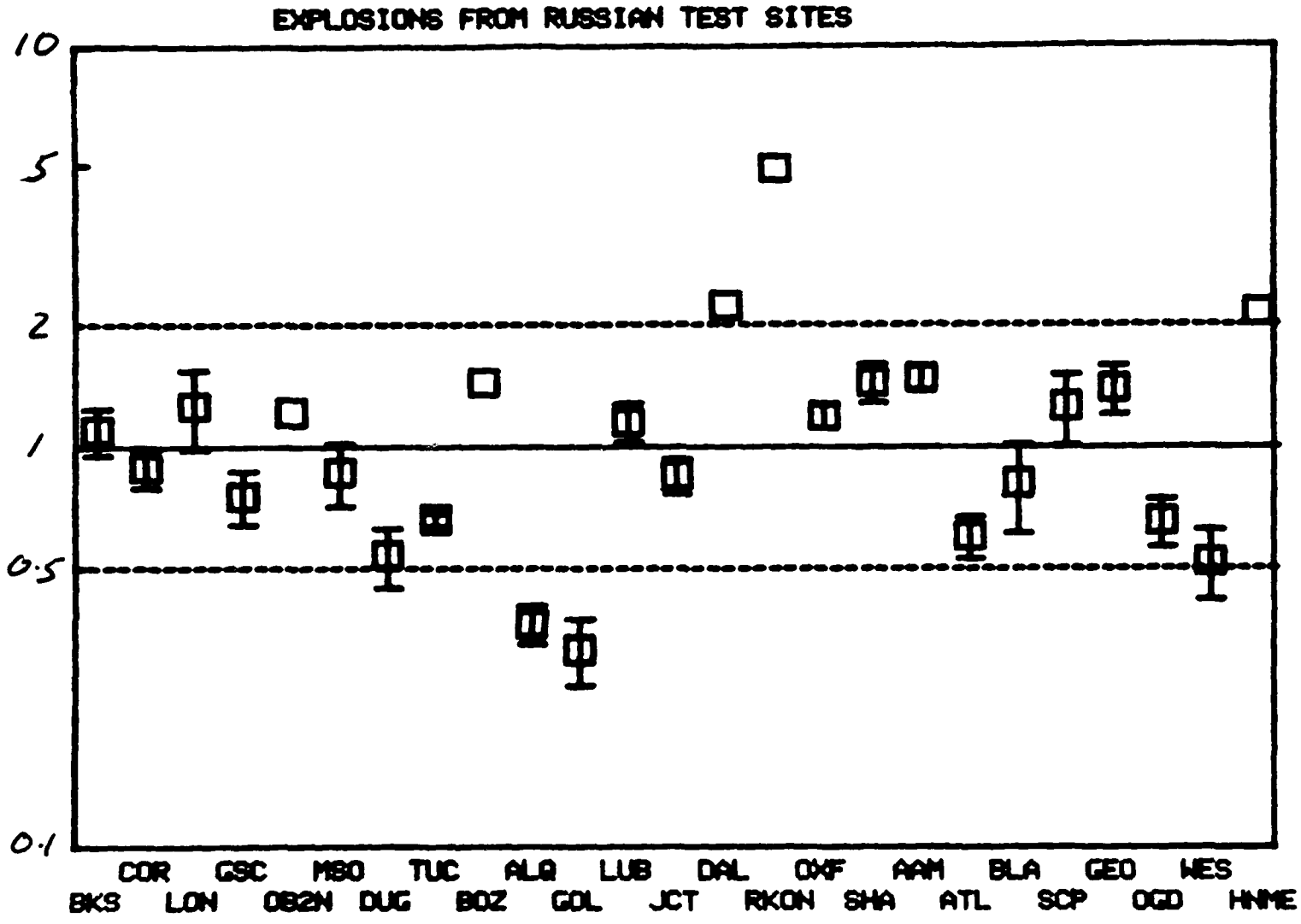
EXPLOSIONS FROM RUSSIAN TEST SITES
10
5
2
1
0.5
0.1
COR
GSC
MSO
TUC
ALQ
LUB
DAL
OXF
AAM
BLA
GEO
WES
BKS
LON
OB2N
DUG
BOZ
GOL
JCT
RKON
SHA
ATL
SCP
OGD
HNME

Figure 4

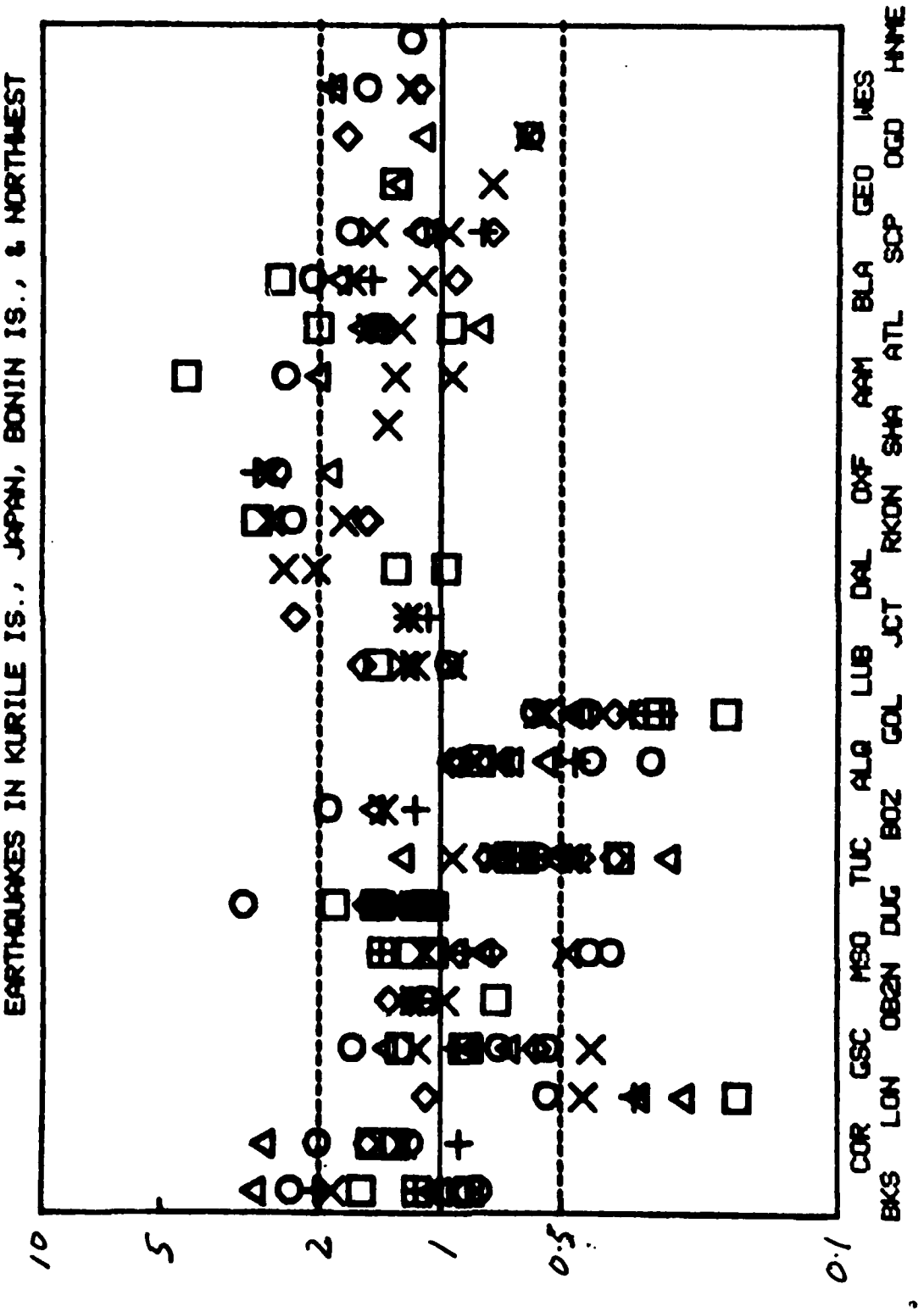
EARTHQUAKES IN KURILE IS., JAPAN, BONIN IS., & NORTHWEST
10
5
2
1
0.5
0.1
BKS LON OBZN DUG BOZ GOL JCT RKON SHA ATL SCP OGD HNME
COR GSC MSO TUC ALQ LUB DAL OXF AAM BLA GEO MES

Figure 5

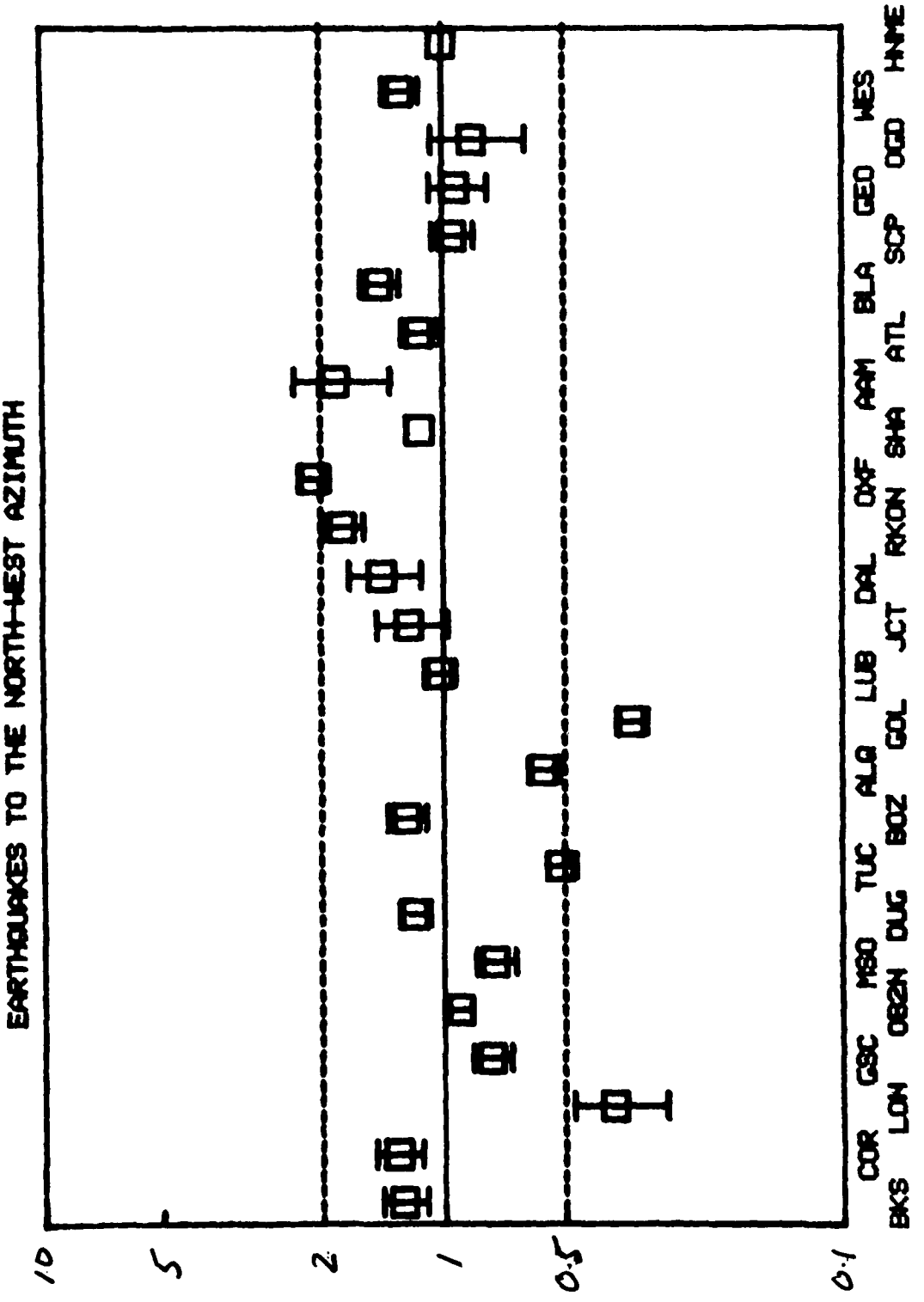
EARTHQUAKES TO THE NORTH-WEST AZIMUTH
10
5
2
1
0.5
0.1
BKS LON OBSN DUG BOZ GOL JCT RKON SHA ATL SCP OGD HNME
COR GSC MSO TUC ALQ LUB DAL OXF AAM BLA GEO WES

Figure 6

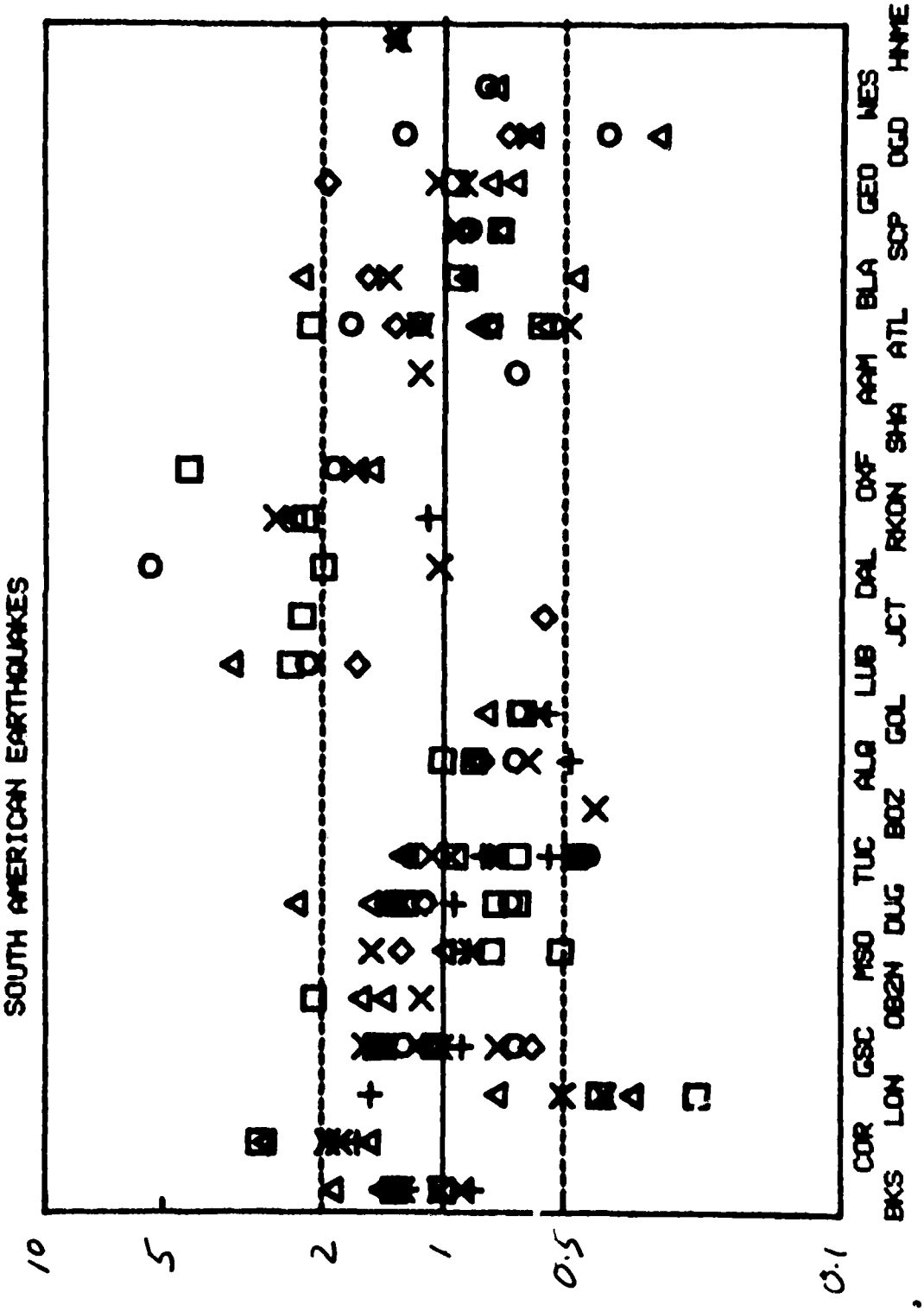
SOUTH AMERICAN EARTHQUAKES
10
5
2
1
0.5
0.1
BKS LON OBZN DUG BOZ GOL JCT RKON SHA ATL SCP OGD HNME
COR GSC MSO TUC ALQ LUB DAL OXF AAM BLA GED NES

Figure 7

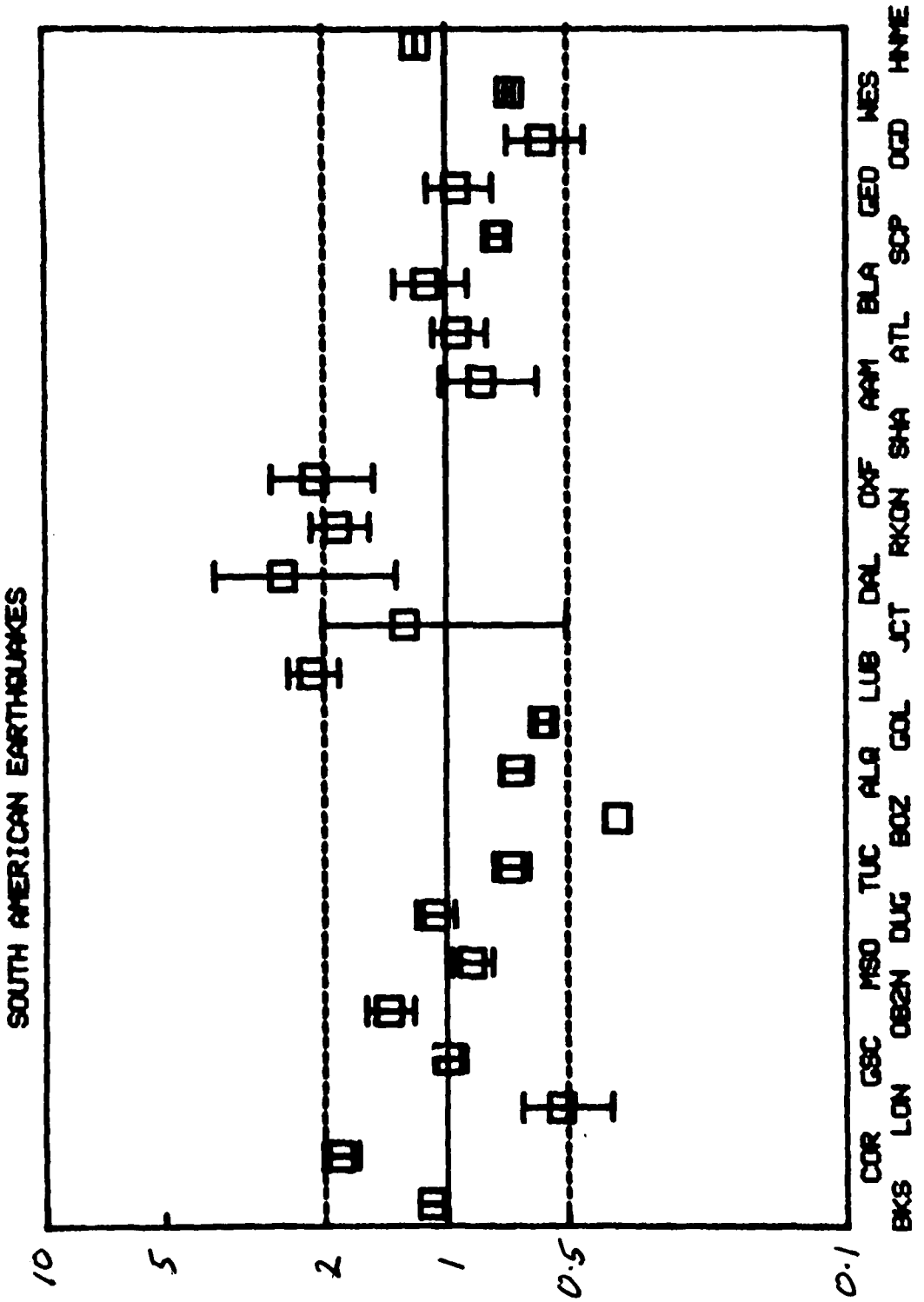
SOUTH AMERICAN EARTHQUAKES
10
5
2
1
0.5
0.1
COR GSC MSO TUC ALQ LUB DAL OXF AAM BLA GED NES
BKS LON OBZN DUG BOZ COL JCT RKON SHA ATL SCP OGD HNME

Figure 8

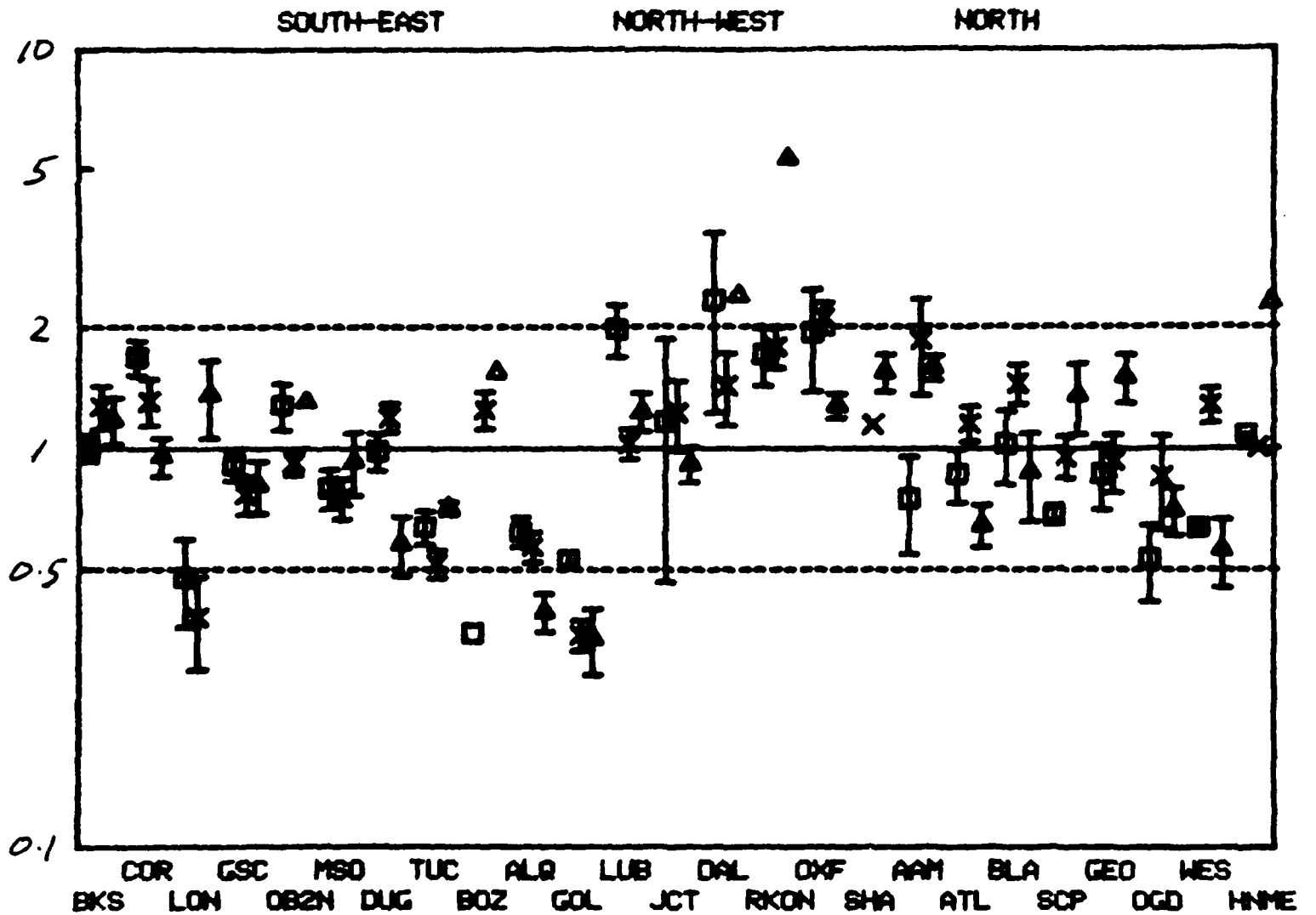

Figure 9. Mean amplitudes for the three azimuth windows. (Trianple - N; Square - SE; and X - NW.)

western stations do not show significant differences. One possible explanation may be the importance of sediment amplification (see Butler, 1979). In all of these compilations, no correction has been made for this effect. The central midwest also represents by far the most significant sedimentary thicknesses for any of these WWSSN stations. The magnitude of this correction would be 1.5-2.0. Application of such a factor would uniformly reduce the amplitude at these stations for all azimuths.

Figure 9 plots the station means for all three azimuths together. The most prominent feature apparent in this figure is the somewhat higher amplitudes observed for the central midwest. Again, sediment amplification corrections would reduce this feature. However, it is interesting to consider what the overall geological or geophysical significance of this phenomenon may be. The utility of such a consideration is the possibility that we might gain some additional insight into the potential advantages or disadvantages of proposed monitoring sites inside Eurasia. Figure 10 is a particularly good illustration of the observed amplitude variations across the United States. In this figure the size of the amplitude anomaly at each station is shown by the size and "polarity" of three triangles, one for each azimuth.

To this end, we have attempted to catalogue many of the major geological and geophysical parameters associated with each station and have looked for correlations between those parameters and the observed amplitude variations. In particular, we have examined these data sets for correlations with the three most prominent amplitude features, the exceptionally low amplitudes of stations ALQ and GOL, the abrupt transition from the relatively low amplitude stations DUC, TUC, BOZ, ALQ and GOL to the high amplitude stations LUB, JCT and DAL, and the high amplitudes in the central midwest. These geophysical data are presented in Figures 11 - 19, each of which is discussed briefly below.

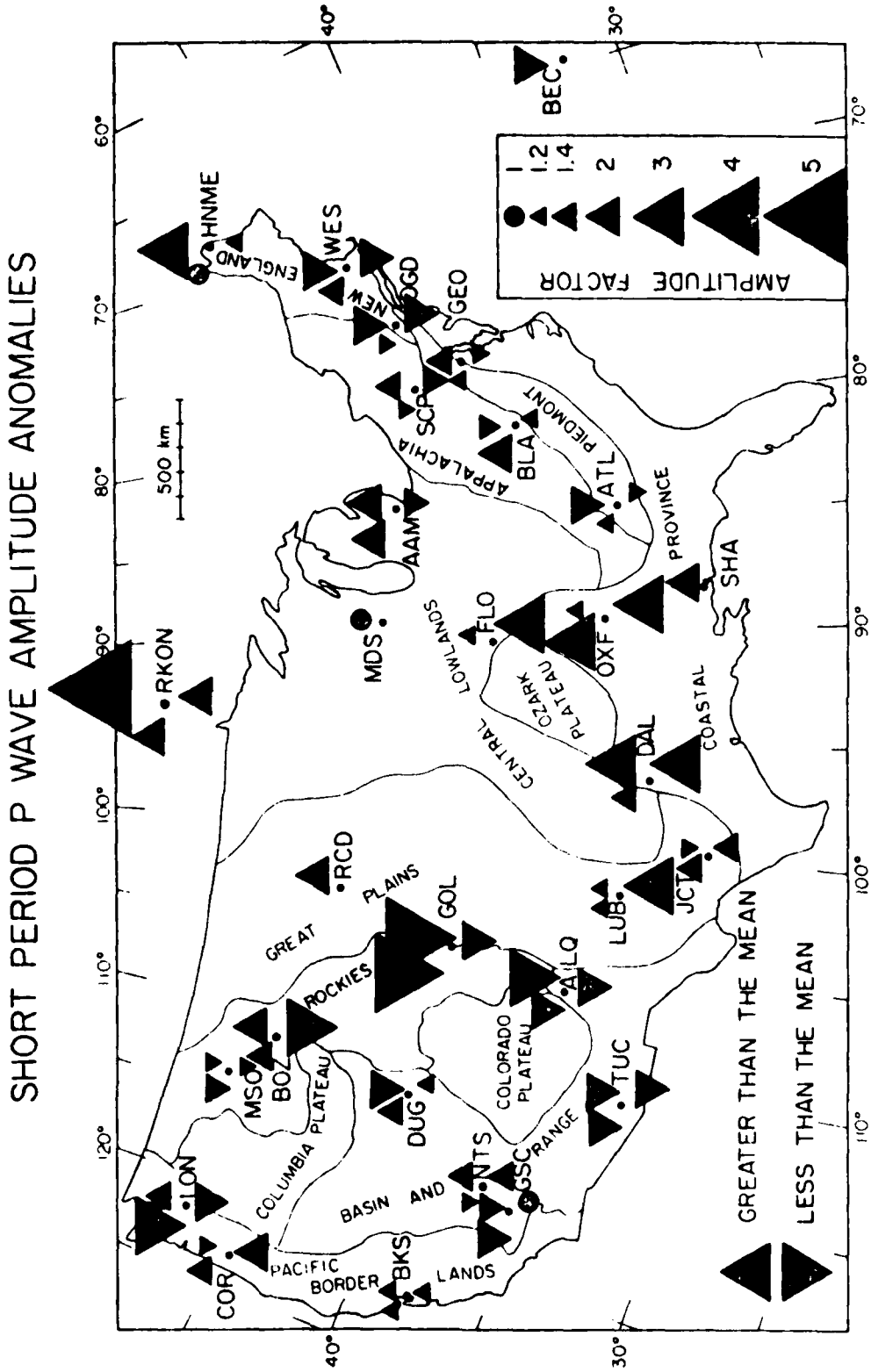
SHORT PERIOD P WAVE AMPLITUDE ANOMALIES
AMPLITUDE FACTOR
1
1.2
1.4
2
3
4
5
GREATER THAN THE MEAN
LESS THAN THE MEAN
500 km
BEC
HNME
ENGLAND
WES
NEW
LOGD
GEO
SCP
BLA
ATL
PIEDMONT
APPALACHIA
PROVINCE
SHA
AAM
MDS
RKON
FLO
OXF
LOWLANDS
OZARK PLATEAU
CENTRAL
DAL
COASTAL
RCD
PLAINS
GOL
GREAT
ROCKIES
LUB
JCT
ALQ
COLORADO PLATEAU
TUC
MSO
BOZ
DUG
COLUMBIA PLATEAU
LON
COR
PACIFIC BORDER
BKS
BASIN AND RANGE
NTS
GSC
120°
110°
100°
90°
80°
70°
60°
40°
30°

Figure 10

Figure 11 plots relative P-wave travel-time residuals. No particular correlation with the observed amplitudes is apparent either in this data or in the residual corrected to a standard (33 Km) crustal thickness (Figure 12). The correlation is also insignificant between S residuals corrected for crustal thickness, Figure 13. The relative S-residuals, Figure 14 (Hales and Roberts, 1970), show a slight correlation with the amplitude data, with slow travel-times correlation with low amplitudes. However, this correlation is not particularly striking as 25% of the stations deviate significantly from the trend. P_n velocities (Herrin, 1969; Mereau and Hunter, 1969), Figure 15, do start to show trends more like some of those found in the amplitude data. The P_n data exhibits a sharp break at the Rocky Mountain front changing from a relative constant value of about 8.1 across the eastern U. S. to a roughly linear decrease to about 7.8. However, while this does correlate with the Rocky Mountain front, it fails to correlate with the amplitudes at ALQ and GOL or across the central midwest. Moreover, the amplitude behavior at the other western stations is the same as that observed for the eastern U. S., while P_n velocity is quite different for those areas.

Heat flow (Diment et al. 1976), Figure 16, also exhibits a sharp break at the Rocky Mountain front but once again, that is the only noticeable correlating feature. Crustal thickness, Figure 16, shows a similarly poor correlation with the amplitude data. An additional non-seismological parameter is electrical conductivity. Figure 17 plots relative conductivity data from Gough (1974) for the western U. S. stations. The most promising feature of this data set is the apparently high conductivity at ALQ and GOL.

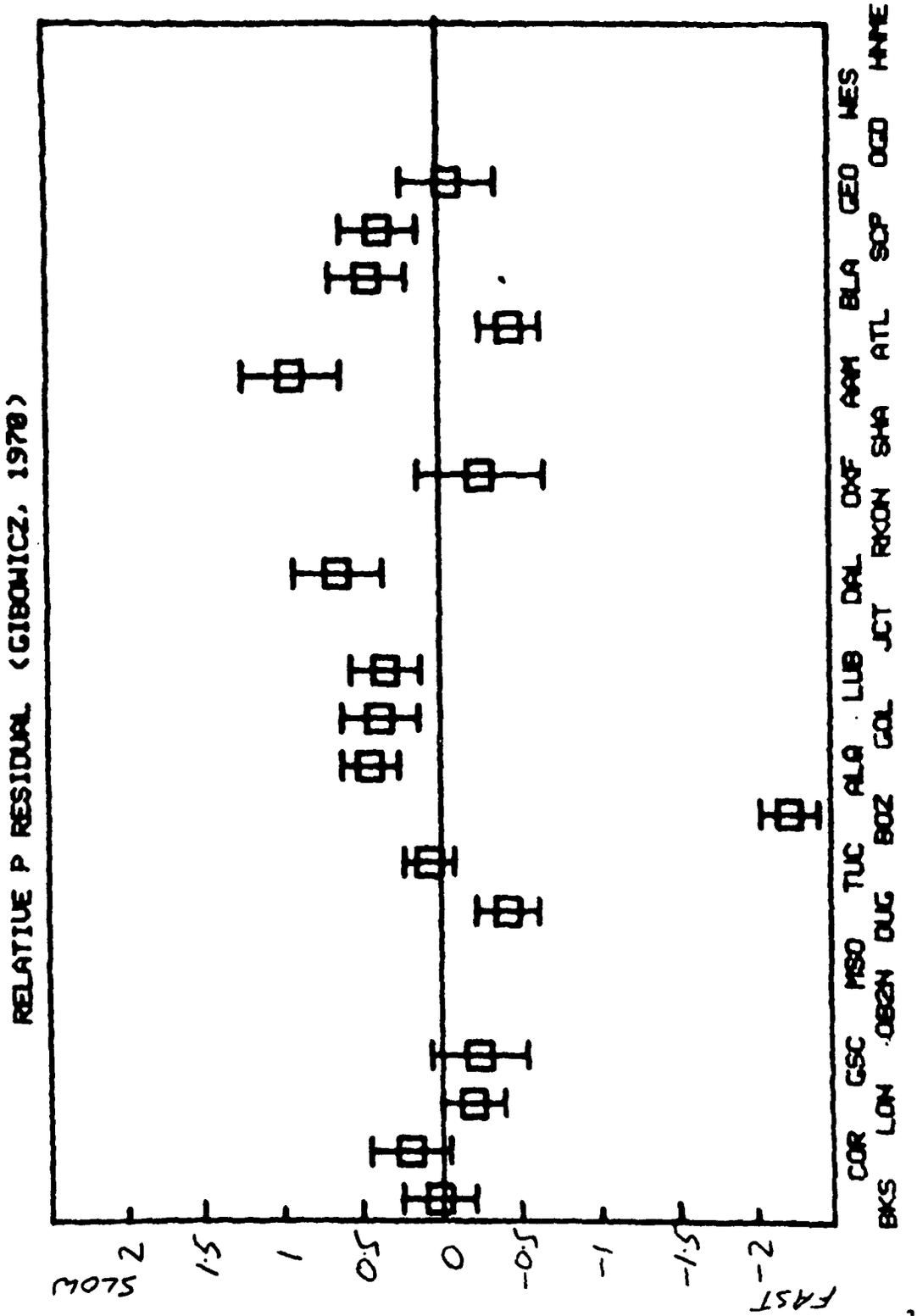
RELATIVE P RESIDUAL (GIBOWICZ, 1978)
SLOW
FAST
2
1.5
1
0.5
0
-0.5
-1
-1.5
-2
BKS LON OBZN DUG BOZ COL JCT RXON SHA ATL SCP OGD HNME
COR GSC MSO TUC ALQ LUB DAL OKF AAM BLA CEO MES

Figure 11

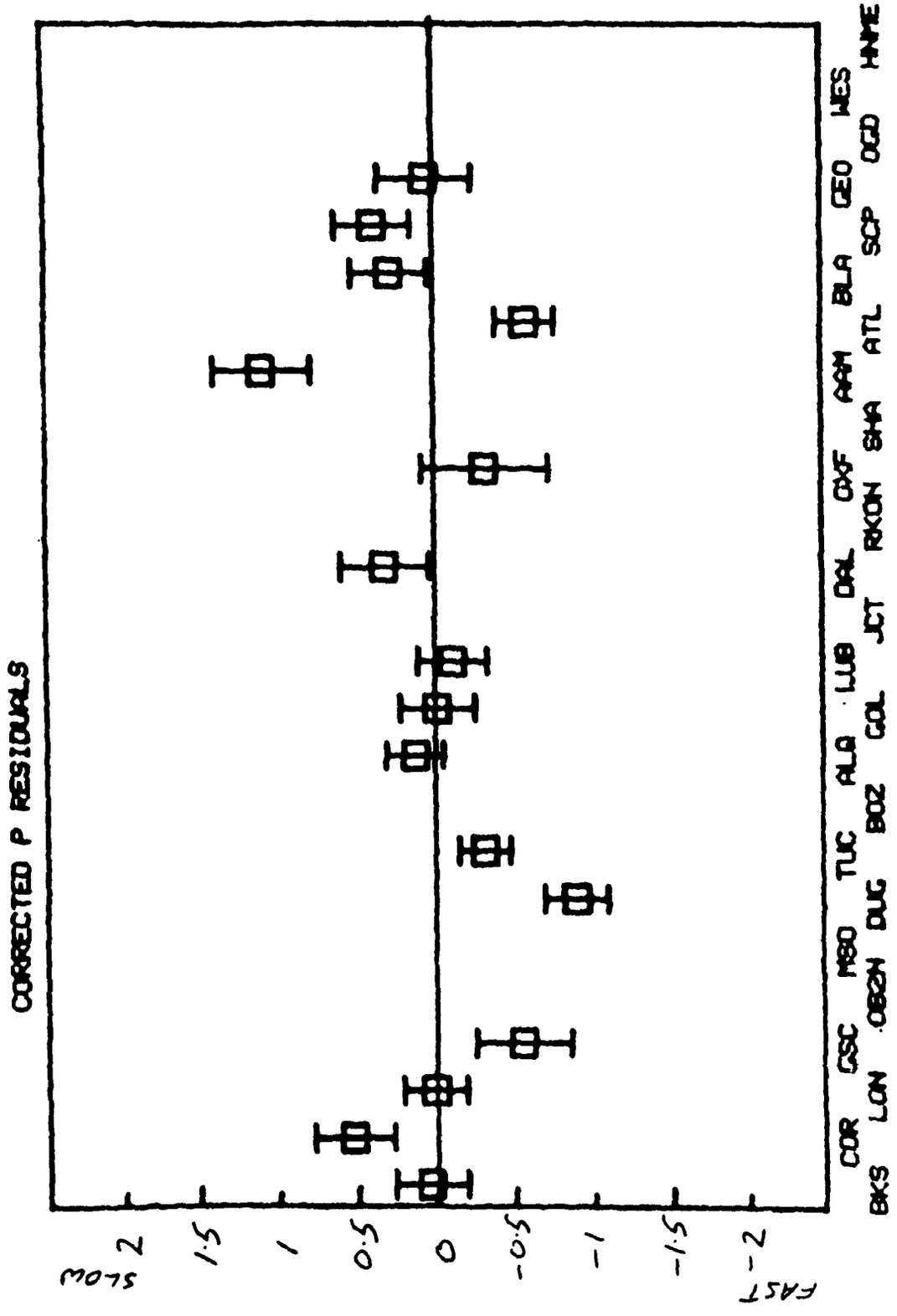
CORRECTED P RESIDUALS
SLOW
FAST
2
1.5
1
0.5
0
-0.5
-1
-1.5
-2
BKS LON OBSN DUG BOZ GOL JCT RKON SHA ATL SCP OGD HNME
COR GSC MSO TUC ALQ LUB DAL OXF ANN BLA GEO WES

Figure 12

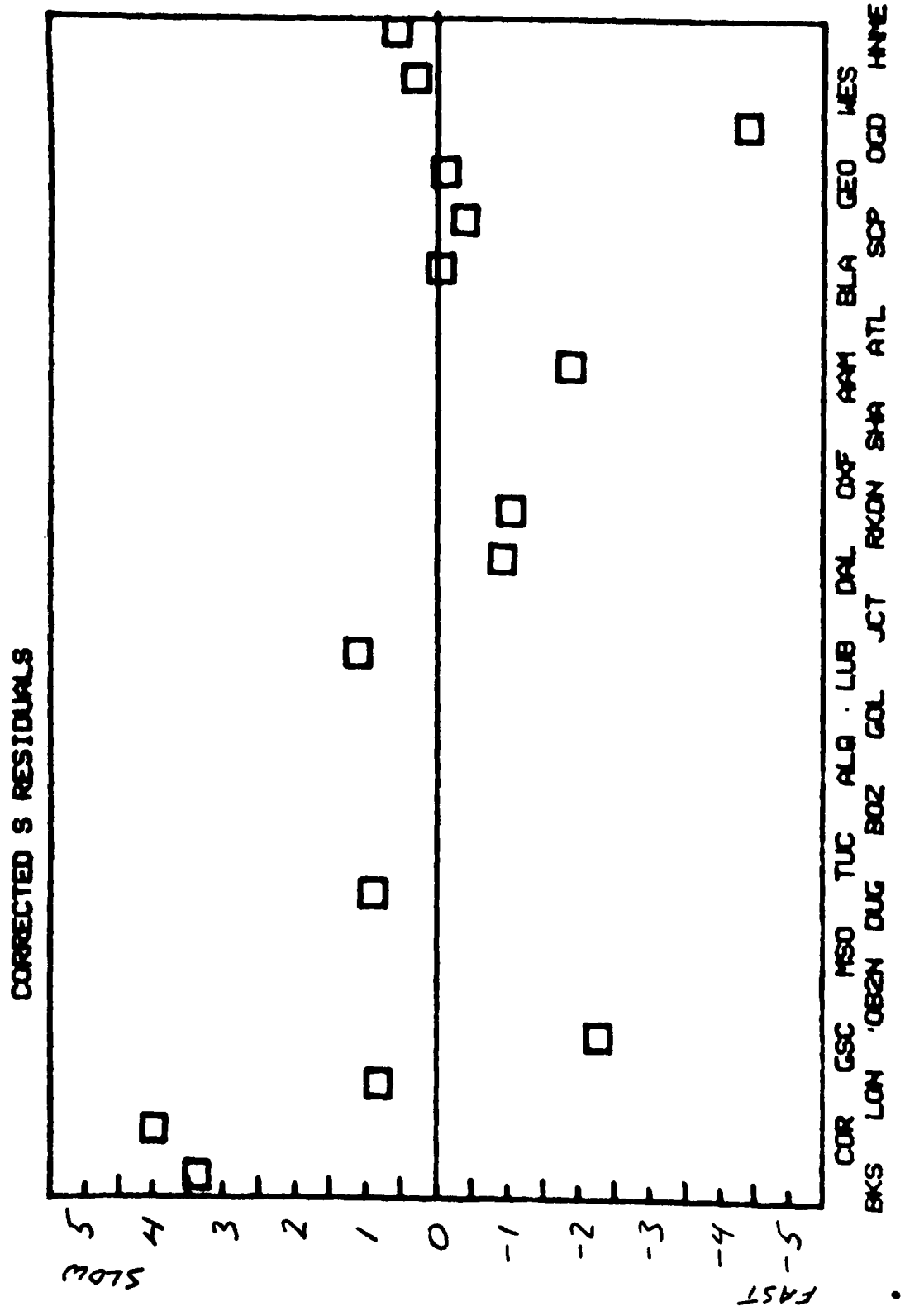
CORRECTED S RESIDUALS
SLOW
FAST
5
4
3
2
1
0
-1
-2
-3
-4
-5
BKS LGN 'OBSN OLG BOZ GOL JCT RKON SHA ATL SCP OGD HNME
COR GSC MSO TUC ALQ LUB DAL OKF AAM BLA GEO WES

Figure 13

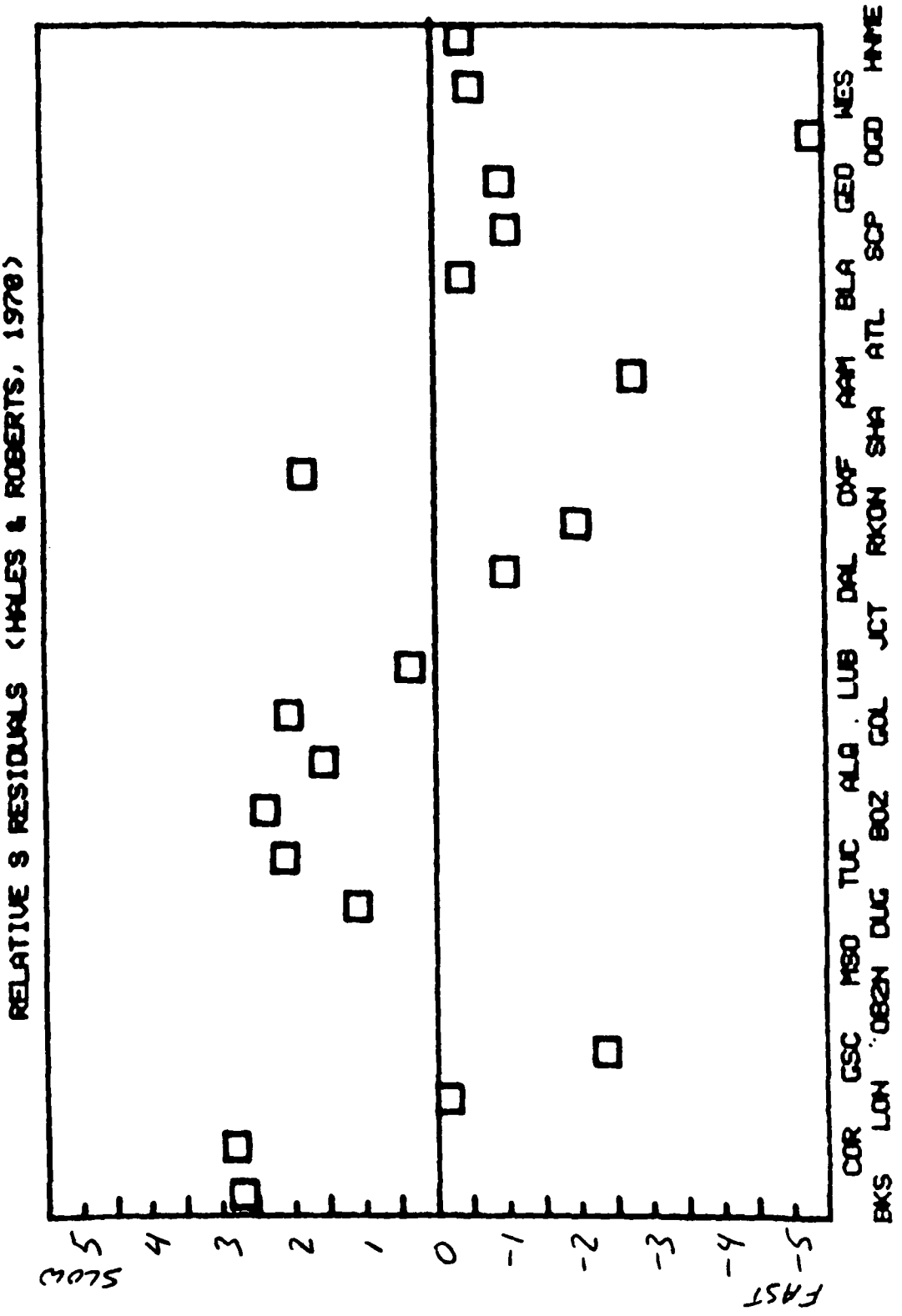
RELATIVE S RESIDUALS (HALES & ROBERTS, 1970)
SLOW
FAST
5
4
3
2
1
0
-1
-2
-3
-4
-5
COR GSC MSO TUC ALQ LUB DAL OKF AAM BLA GED WES
BKS LON OBSN OLG BOZ GOL JCT RKON SHA ATL SCP OGD HNME

Figure 14

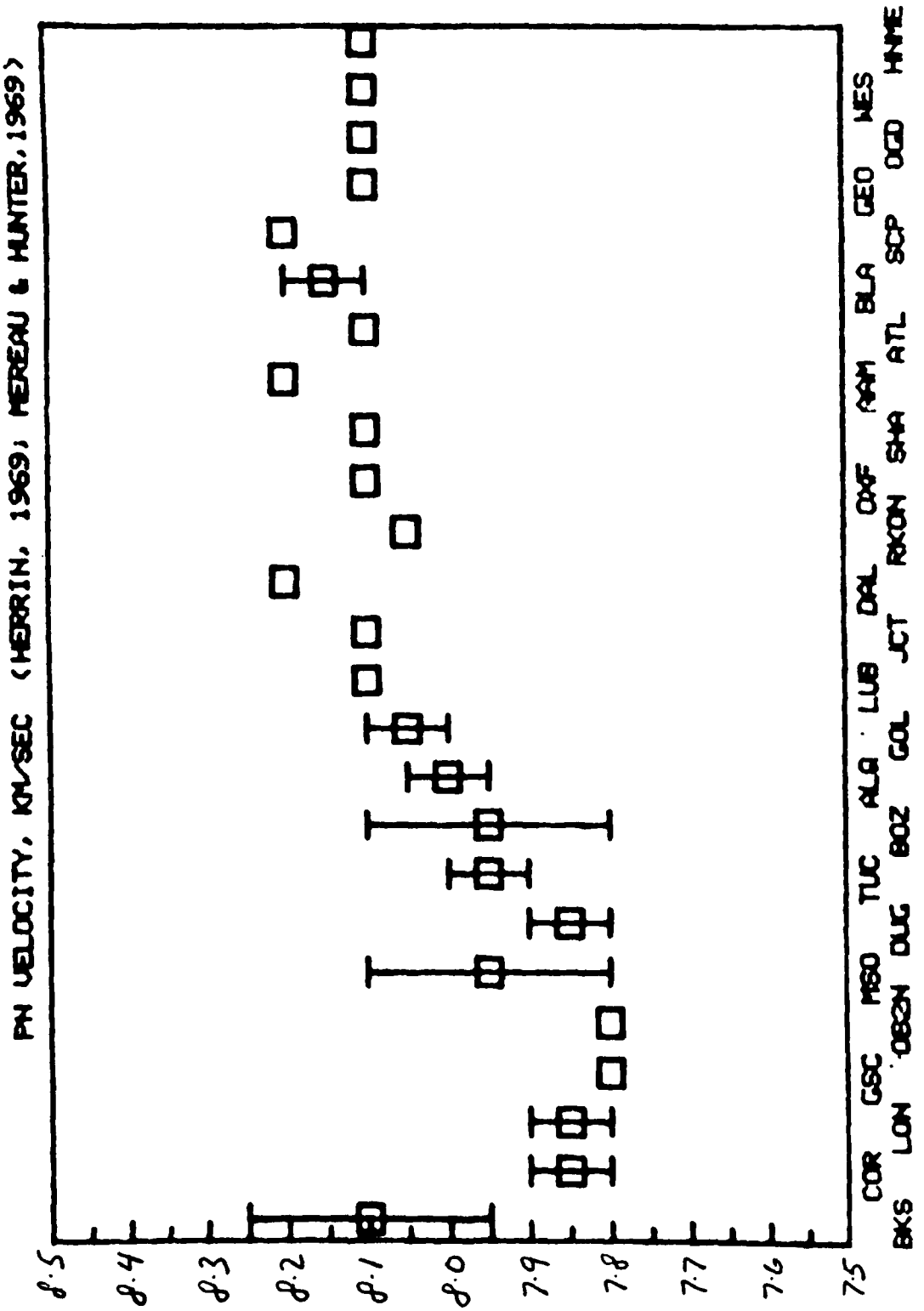
PN VELOCITY, KM/SEC (HERRIN, 1969; MEREAU & HUNTER, 1969)
8.5
8.4
8.3
8.2
8.1
8.0
7.9
7.8
7.7
7.6
7.5
BKS LON OBSN DUG BOZ GOL JCT RXON SHA ATL SCP OGD HNME
COR GSC MSO TUC ALQ LUB DAL OXF ANM BLA GEO MES

Figure 15

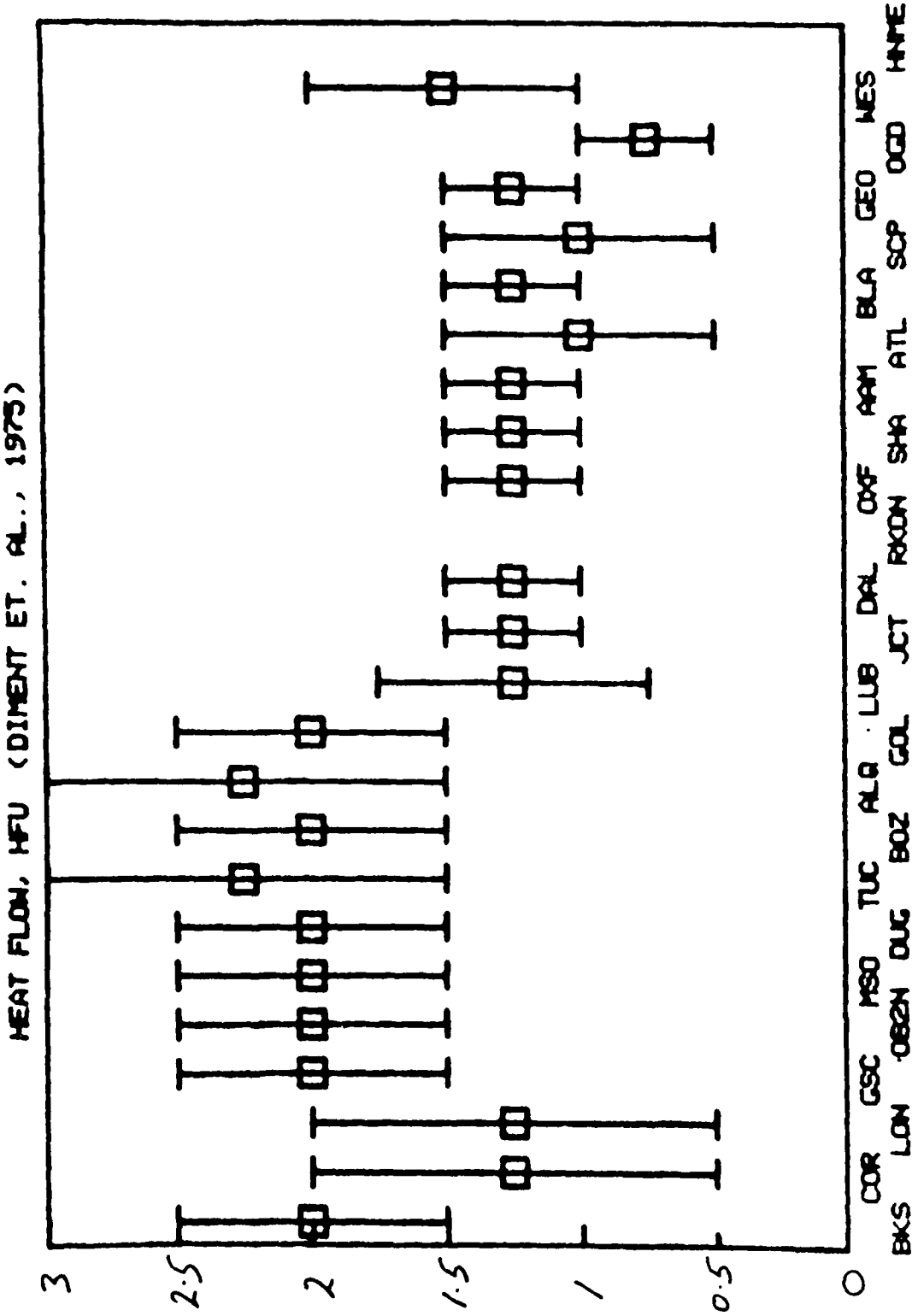
HEAT FLOW, HFU (DIMENT ET. AL., 1975)
3
2.5
2
1.5
1
0.5
0
BKS LON OBGN DUG BOZ COL JCT RXON SHA ATL SCP OCD HNME
COR GSC MSO TUC ALQ LUB DAL OXF ANN BLA GEO MES

Figure 16

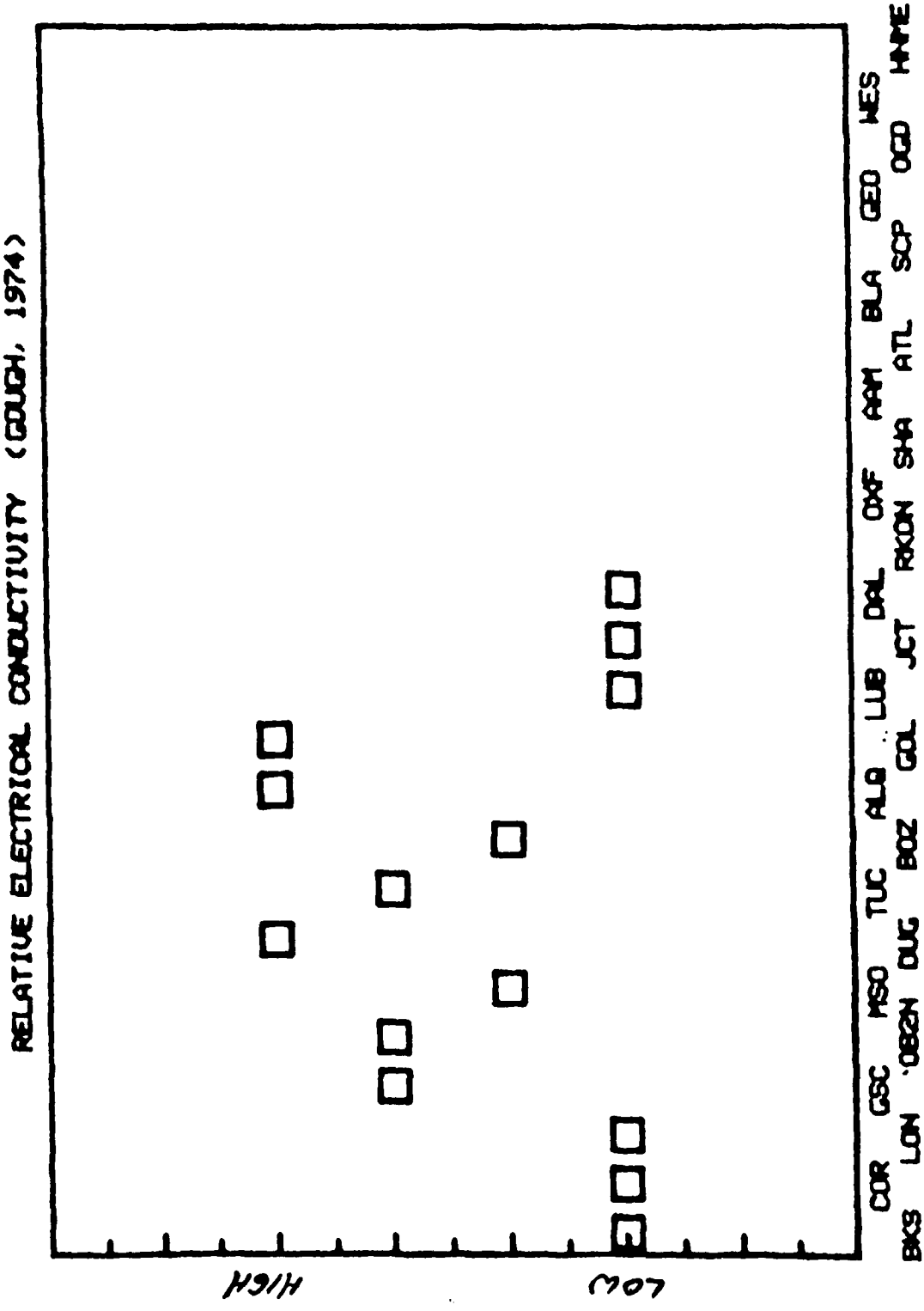
RELATIVE ELECTRICAL CONDUCTIVITY (COUCH, 1974)
HIGH
LOW
COR GSC MSO TUC ALQ LUB DAL OKF AAM BLA CED MES
BKS LON OBSN DUG BOI COL JCT RKON SHA ATL SCP OCD HAME

Figure 17

The last two parameters to be discussed here are Bouguer gravity (Figure 18), and station elevation (Figure 19). In this simple comparison of various geophysical parameters, gravity and station elevation (high elevation with low amplitudes) correlate best with the observed amplitude pattern. However, the high amplitudes discussed above for stations in the central U. S. do not correlate with high gravity and several low elevation stations show mean amplitudes. The approximate correlation of both gravity and station elevation with the amplitude data is almost certainly not a coincidence. Many investigators have noted the frequent strong correlation between Bouguer gravity and elevation. Indeed, many of the geophysical parameters discussed above are interrelated. For instance, Crough and Thompson (1976) has proposed a mechanism for interrelating crustal thickness, heat flow and elevation. Such interdependence of one parameter upon another may obscure simple correlations. For instance, correcting P-delays for station elevation or crustal thickness, although both reasonable and necessary, may further cloud the relationship between amplitude or m_b bias and crustal thickness.

The obvious next step is a more mathematically formal comparison of these parameters to evaluate if a true correlation exists. This task will be undertaken in the near future.

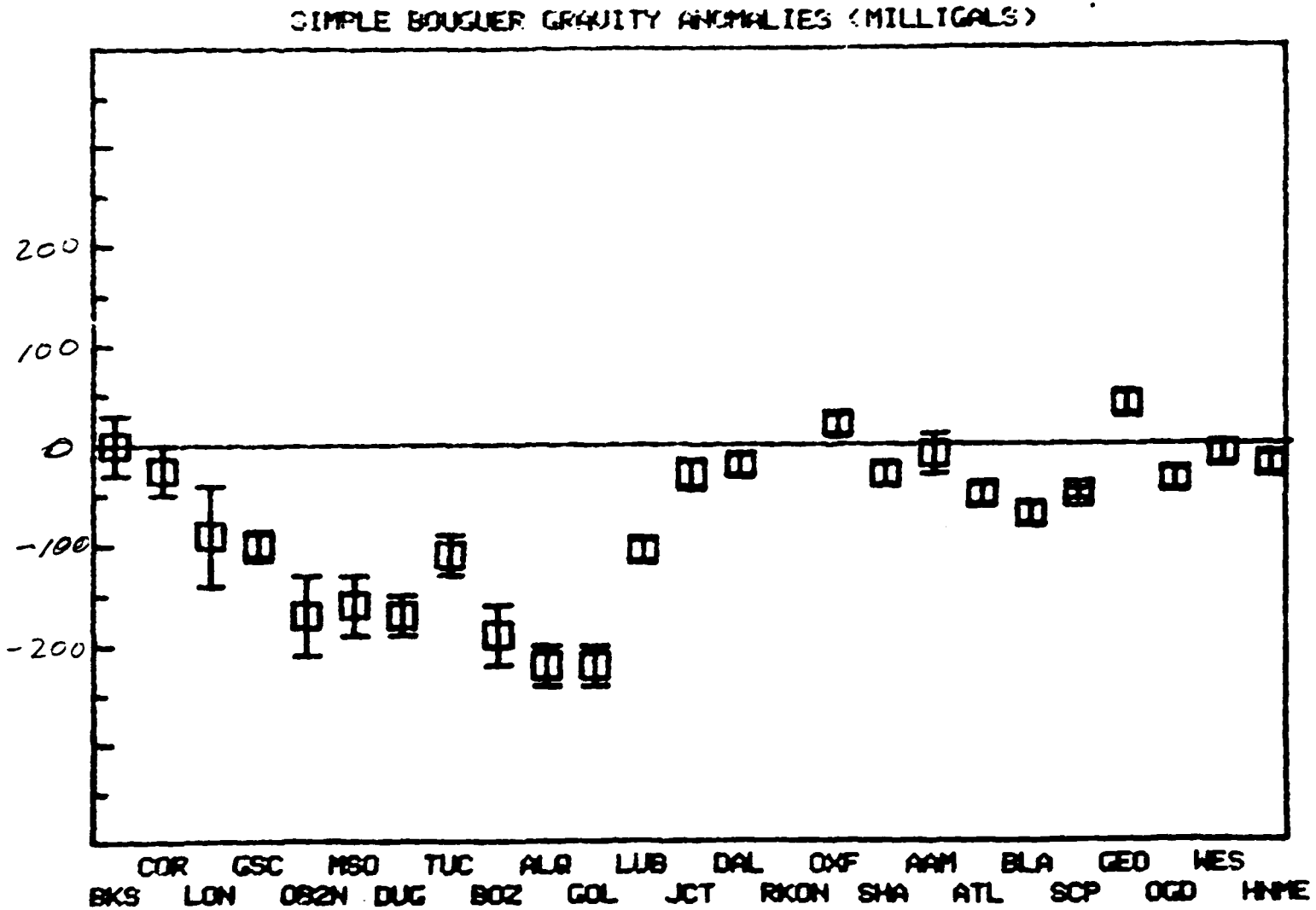
SIMPLE BOUGUER GRAVITY ANOMALIES (MILLIGALS)
200
100
0
-100
-200
COR
GSC
MSO
TUC
ALQ
LUB
DAL
OXF
AAM
BLA
GED
WES
BKS
LON
OBZN
DUG
BOZ
GOL
JCT
RKON
SHA
ATL
SCP
OGD
HNME

Figure 19

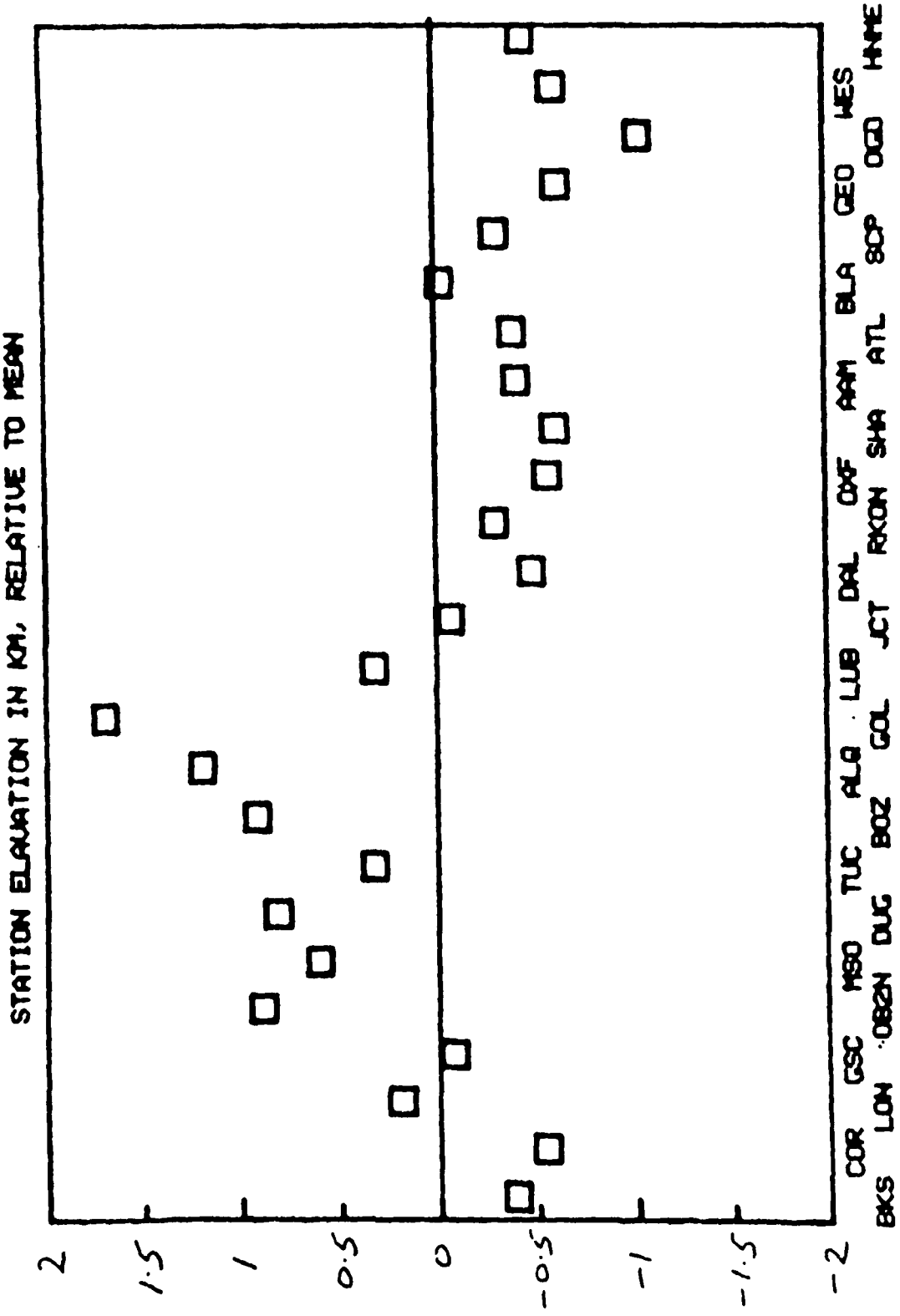
STATION ELAVATION IN KM, RELATIVE TO MEAN
2
1.5
1
0.5
0
-0.5
-1
-1.5
-2
COR GSC MSO TUC ALQ LUB DAL OKF AAM BLA CEO WES
BKS LOW OBSN DUG BOZ GOL JCT RKON SHA ATL SCP OCD HNME

Figure 19

III. STATION TRANSPARENCY

In performing waveform fitting and inversion studies, it is important to minimize or eliminate effects other than those being modeled. Often experiments are designed specifically to eliminate certain effects, such as using data in the 30 to 90 degree range for source studies in order to suppress propagation effects. Certain other effects are not easily modeled or suppressed. One such is the effect of near-receiver structure on incoming waveforms.

The method most commonly used to deal with near-receiver structure is to exclude data from non-transparent stations. The decision as to whether a station is sufficiently transparent or not is generally purely subjective on the part of the investigator. In general, if a station repeatedly exhibits complex waveforms for events that appear simple at other stations, that station is rejected as being "non-transparent." Waveform complexity may take the form of excessive ringing in the record, or of distinct, isolated arrivals which appear for all events.

One method for studying the effects of near-receiver structure is to examine particle motion as a function of time for P-waves of simple events recorded at a given station. Since reflections from dipping and non-planar interfaces will in general either contain significant S-wave energy or arrive from a different direction than will the direct P-wave, a change in the direction of particle motion indicates the presence of such structures. This method has been used by Burdick and Langston (1977) to study selected WWSSN stations.

While this method does give an indication of the time window available before the arrival of significant reflections from non-flat structures, it

is not, in general, effective in identifying arrivals from flat layered structure, nor does it provide a method of correcting observed seismograms for the effects of near-receiver structure. Moreover, three-component data are necessary for this method, and these are not available in many instances.

Another approach to identifying transparent stations is to use a quantitative measure of waveform complexity on the vertical components of several stations. One such measure of complexity is provided by the varimax norm

$$V = \frac{\int \chi^4(t)dt}{(\int \chi^2(t)dt)^2} \qquad (1)$$

This function has had extensive use in econometrics and has been used in geophysical applications by Wiggins (1978) as a measure of simplicity in the Minimum Entropy Deconvolution (MED) method. The varimax norm has a maximum of 1 for a delta function, and decreases as the complexity of the function increases. It is sensitive only to the number and relative amplitude and width of arrivals, and not to absolute amplitudes or relative arrival times. For a more complete discussion of the properties of the varimax norm, see Wiggins (1978).

The varimax norms for a ten-second time window for a number of events recorded at SDCS stations OB2-NV, YF1-NV, YF2-NV, YF3-NV, and YF4-NV are shown in Table 28. Station OB2 is located in a granitic stock, while stations YF1-YF4 are located in an alluvial basin. As may be expected, seismograms recorded at OB2 for simple events appear significantly more simple than do those recorded at the YF stations.

TABLE 28

Event	OB2	YF1	YF2	YF3	YF4
772505	.055	.018	.022		
771706	.052	.023	.026	.018	.021
772106	.042	.015	.017		
770506	.041	.015	.014	.013	.016
772407	.035	.013	.014	.012	.017
771706	.033	.013	.014		
771508	.022	.019	.020	.012	.015
770309	.021	.016	.016	.014	.021
772907	.019	.013	.015	.015	.013
771306	.019	.013	.016		
772907	.019	.018			
771319	.014	.014	.013		.017
772407	.011	.012	.012		

Table 28 shows varimax norms for a number of events, ordered by the value of the norm for OB2. As may be seen, the value of the norm does not excede ~.025 for any event for any of the YF stations, while the value for OB2 may be as high as .05. This may be interpreted as an indication that the complexity of the receiver function maintains the relatively low values of the norms for the YF stations even for simple sources. As the complexity of the source increases, this increase is shown by a decrease in the norm for OB2, while the norms for the YF stations show little change until such time as source complexity exceeds receiver function complexity. For highly complex sources, the interaction of the source with the complicated receiver functions at the YF stations may produce slightly higher norm values at some YF stations than at OB2.

Thus use of the varimax norm may be seen to provide some quantitative rating criterion for single-component stations. It requires, however, simple sources that are stationary from station to station and a high signal to noise ratio to give meaningful results. While the method gives useful results, it does not provide any method for correcting data for near-receiver effects nor of estimating the effects of receiver structure on waveform fits. Such information may be obtained only by obtaining an estimate of the receiver function.

A method for estimating receiver functions by deconvolution, log spectral stacking and Minimum Entropy Deconvolution has been developed by Hadley and Mellman. Details of this method, together with applications to stations OB2-NV and YF1-YF4-NV are given in Hart et al. (1979). Future research will involve use of this method to derive receiver functions for a number of commonly used stations.

IV. SHORT PERIOD WAVEFORM INVERSION FOR NUCLEAR SOURCE TIME FUNCTIONS

The conventional technique for determining the teleseismic time function of nuclear events is by matching synthetic seismograms with the observed records: varying the source parameters, the depth of burial, and possibly t* until a satisfactory match is obtained. Instead of applying this trial-and-error subjective method, we are developing a formal waveform inversion technique which will allow for an investigation of uniqueness of the source parameter determination and can potentially be used for systematic estimation of source parameters.

Long period instruments can provide some important constraints, but, in general, short period instruments are more useful for distinguishing the values of the three source parameters; rise time, overshoot, and time delay of the free surface reflection. The trade-off between these three parameters which produces similar seismograms is not well explored, and it is clearly desirable to know if a rather large number of parameter combinations result in nearly the same seismogram. A formal inversion procedure to determine the source parameters from a seismogram can be used to investigate this nonuniqueness. Also, if the inversion method proves to be relatively stable in the parameter estimates, then the time functions of nuclear events can be estimated systematically utilizing a simple description of the waveforms.

Additionally, if the method does prove to be reliable, an inversion using a worldwide network could be a simple but effective discriminate for nuclear events.

The essential idea in the method employed is that for short period records a satisfactory match between two seismograms is simply obtained when the relative peak heights and the corresponding time separation of the peaks are the same. This is easily verified to be the case except when there are distinct inflections in the waveform. Given this numerical definition of the waveform, the inversion procedure is quite simple. As the source parameters occur in a non-linear relationship, the inversion works as an iterative process as follows: (1) Initial values of the parameters are given, (2) a synthetic seismogram is then constructed and compared to the data, resulting in an error vector. (3) If the error is not acceptable, then perturbations to the parameters are calculated. With the new parameter values, return to step (2).

The basic software for this formal inversion has been developed and some preliminary results have been obtained regarding the stability of the method. Figure 20 shows the results of a test with artificial data. The dashed seismogram is constructed from a cosine interpolation of the input peak amplitudes and times. In this example, the amplitudes and times were taken from a synthetic seismogram using a von Seggern-Blandford, (1972) source function with the parameters: R(1/Rise Time) = 5.0, OV (over-shoot parameter) = 2.0, and TPP (time lag of pP) = 0.5 sec. After just two iterations, the seismograms are in excellent visual agreement. Allowing the program to continue, after a total of five iterations, the artificial data was "inverted" to the parameter values: R = 5.07, OV = 2.00, and TPP = 0.50. It is of interest to note that the program approached the final values in a monotonic manner. Results like this indicate that the convergence will be smooth over a wide range of source parameter values. The smoothness with respect to pP delay time has not yet been investigated.

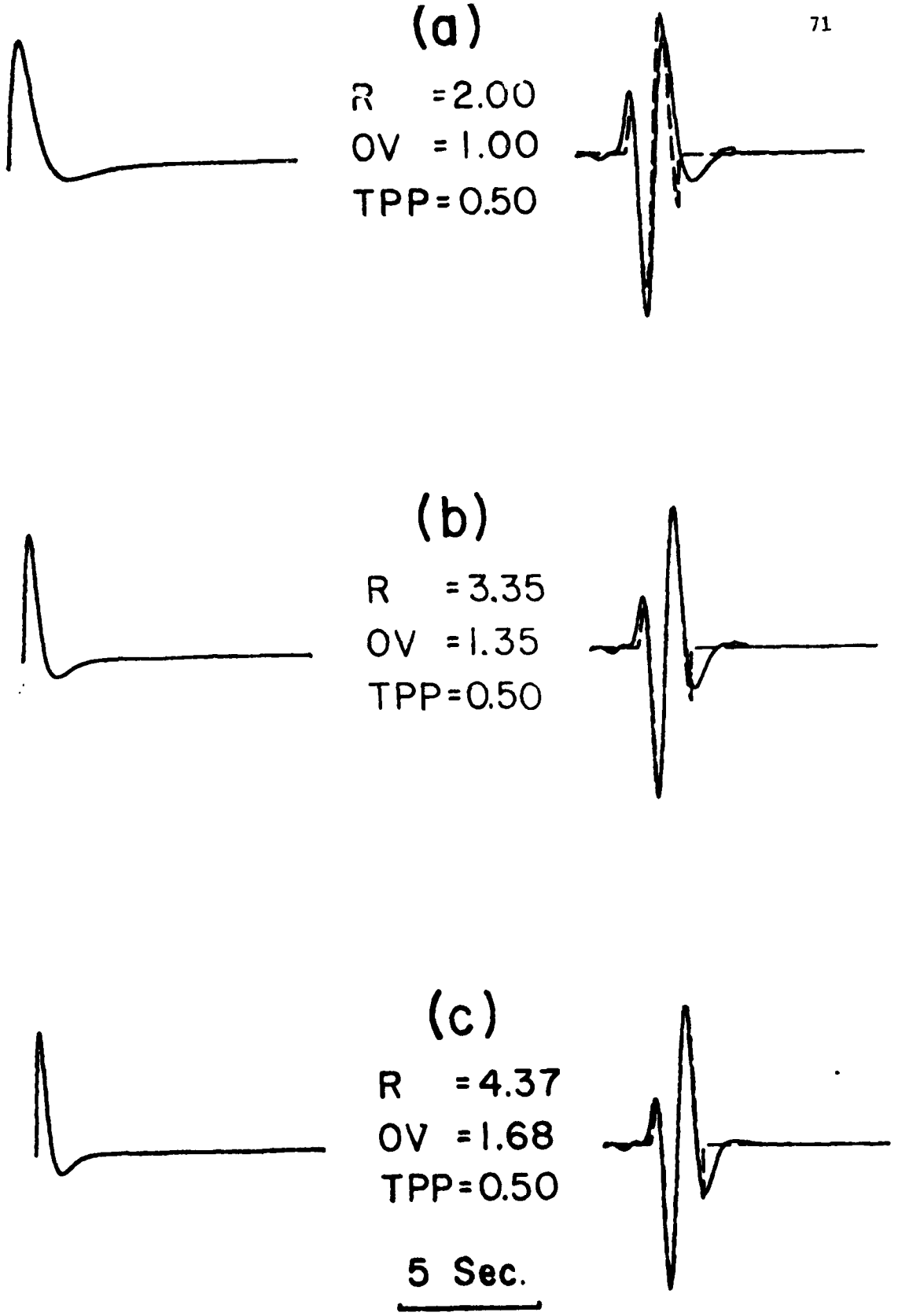

Figure 20. An inversion test to retrieve the source parameters of synthetic data. The dashed seismogram in (a), (b), and (c) is constructed from a synthetic using t*=1.0, R=5.0, OV=2.0, TPP=0.50. The initial input trial source and the resultant synthetic are shown in (a), with (b) and (c) showing the results of the first two iterations respectively. As can be seen there is an excellent visual correspondence after just two iterations.

One of the major uses of this method will be examining the tradeoff between source parameter variations and errors in the data: Figure 21 presents a test case for that problem. *The dashed seismogram is the same* as in Figure 20 except that the fourth peak amplitude has been arbitrarily reduced to 1/2 of its original value, perhaps mimicking an error caused by receiver structure. As seen in Figure 21, if the peak amplitudes and times are used in the inversion, the parameters are tightly constrained and after four iterations there is virtually no change. However, if only the peak amplitudes are used as data, the problem is just barely over-determined and consequently there is quite an adjustment to the parameters. Figure 21 shows that after four iterations the changes in the parameters has reduced the error of the fourth peak from 100% to 50%. Studies such as this test will further our understanding of how errors in the data can be mapped into errors of the source parameters.

To conclude with the current status of this inversion method, the progress thus far has been to verify that the numerical parameterization of the waveform is appropriate and useful, and to develop the basic software for the formal inversion with a preliminary analysis of stability. Although the entire parameter space has not yet been explored, the smooth convergence using artificial data, encourages the further development of this method as a robust estimator of explosion source functions.

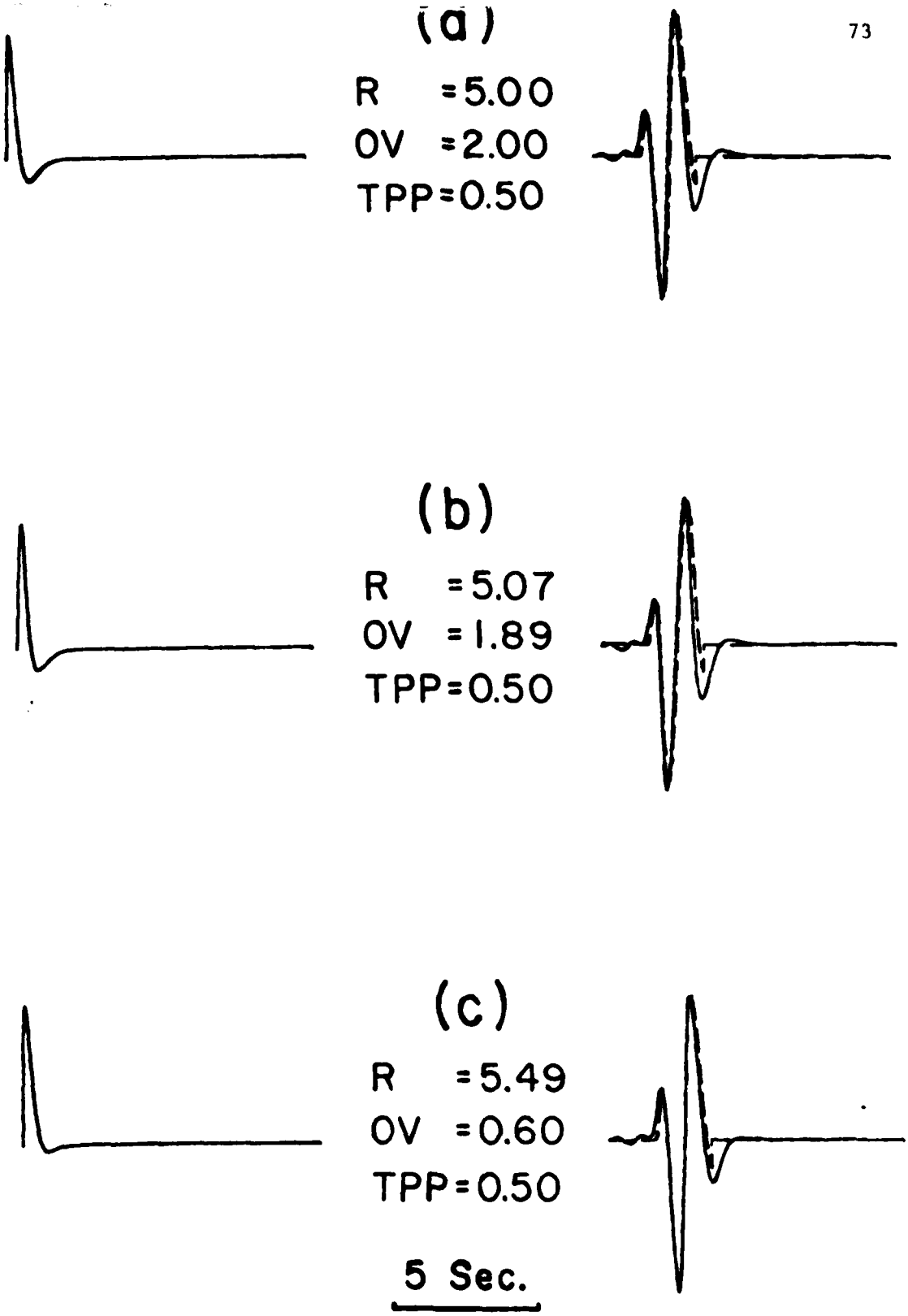

Figure 21. An inversion test introducing arbitrary "noise" to the synthetic data. The dashed seismogram is the same as in Figure 20 except that the fourth peak amplitude is reduced to 1/2 its previous value. The initial source parameters used in (a) are the same parameters used for the synthetic data. The inversion program is then allowed to go through four iterations under two different circumstances: (b) shows the results when using peak amplitudes and peak times as data, and (c) shows the results when using only the peak amplitudes as data.

REFERENCES

Butler, R. (1979), An amplitude study of Russian nuclear events for WWSSN stations in the United States, Sierra Geophysics Technical Report #SGI-R-79-001.

Butler, R., and R. S. Hart (1979), Summary of current research on seismic waveform analysis of underground nuclear explosions, Sierra Geophysics Technical Report #SGI-R-79-004.

Booth, D. C., Marshall, P. D., and J. B. Young (1974), Long and Short period P-wave amplitudes from earthquakes in the range 0°-114°, Geophys. J. R. Astr. Soc., 39, 523-537.

Burdick, L. J. and C. A. Langston (1977), Modeling crustal structure through the use of converted phases in teleseismic body-wave forms, Bull. Seism. Soc. Am., 67, p. 677.

Crough, S. T., and G. A. Thompson (1976), Thermal model of a continental lithosphere, J. Geophys. Res., 81, 4857-4862.

Diment, W. H., T. C. Urban, J. H. Sass, B. V. Marshall, R. J. Munroe, and A. H. Lachenbrunch (1975), Temperatures and heat contents based on conductive transport of heat in Assessment of Geothermal Resources of the United States - 1975, U.S.G.S. Circular 726.

Evernden, J. F. and D. M. Clark (1970, Study of teleseismic P. II amplitude data, Phys. Earth Planet. Int., 4, 24-31.

Gibowicz, S. J. (1970), P-wave travel time residuals from Alaskan aftershocks of 1964, Phys. Earth Planet Interiors, 2, 239-258.

Gough, D. I. (1974), Electrical conductivity under western North America in relation to heat flow, seismology, and structure, J. Geomag. Geoelectr., 26, 105-123.

Hadley, D. M. (1979), Seismic source functions and attenuation from local and teleseismic observations of the NTS events Jorum and Handley, Sierra Geophysics Technical Report #SGI-R-79-002.

Hales, A. L., and J. L. Roberts (1970), Shear velocities in the lower mantle and the radius of the core, Bull. Seism. Soc. Am., 60, p. 1427.

Hart, R. S., D. M. Hadley, G. R. Mellman, and R. Butler (1979), Seismic amplitude and waveform research, Sierra Geophysics Technical Report #SGI-R-79-012.

Herrin, E. (1969), Regional variations in P-wave velocity in the mantle beneath North America, in The Earth's Crust and Upper Mantle, Geophysical Monograph, 13, 242.

Langston, C. A. (1976), Body wave synthesis for shallow earthquake sources: Inversion for source and earth parameters, Ph. D. Thesis, California Institute of Technology, Pasadena, CA.

Mereau, R. F. and J. A. Hunter (1969), Crustal and upper mantle structure under the Canadian shield from Project Early Rise data, Bull. Seism. Soc. Amer., 59, 147-165.

von Seggern, D. and R. Blandford (1972), Source time functions and spectra for underground nuclear explosions, Geophys. J. R. Astr. Soc., 31, 83.

Wiggins, R. A. (1978), Minimum entropy deconvolution, Geoexploration, 16, 21-35.